2010a Paper

The Astrophysical Journal, 714:971–987, 2010 May 1 doi:10.1088/0004-637X/714/1/971

EXPLORING TRANSITIONS OF SPACE PLASMAS OUT OF EQUILIBRIUM

G. Livadiotis[1] and D. J. McComas[1,2]
[1] Southwest Research Institute, San Antonio, TX 78238, USA
[2] University of Texas at San Antonio, San Antonio, TX 78249, USA
Received 2009 November 20; accepted 2010 March 16; published 2010 April 15

ABSTRACT

Space plasmas from the solar wind to planetary magnetospheres and the outer heliosphere are systems in stationary states out of equilibrium. Empirical kappa distributions, which naturally emerge from Tsallis Statistics, successfully describe these space plasmas. The Tsallis formalism offers a solid statistical foundation and provides a set of proven tools for understanding these distributions, including a consistent definition of temperature—the physical temperature, which characterizes the non-equilibrium stationary states. Here, we develop a measure of the "thermodynamic distance" of stationary states away from equilibrium. The stationary states are labeled by the value of the entropic q-index, lying in a spectrum from $q = 1$ (equilibrium) to the maximum value of q, which specifies the furthest possible stationary state from equilibrium. We call this the "q-frozen state," because as a system approaches this state, it behaves analogously to when its temperature approaches absolute zero. We also introduce a novel isothermal procedure that describes a system's transition into different stationary states by varying the q-index, and show how the variation of temperature can be realized using an "iso-metastability" procedure, in which the system remains in a fixed stationary state. These innovations allow a generalization of the zeroth law of thermodynamics to cover stationary states out of equilibrium. By expressing the entropy in terms of the q-index, we show the detailed paths by which the transition of stationary states evolves toward equilibrium following the dynamics of a characteristic difference equation along the q-indices. This naturally exhibits certain stationary states out of equilibrium that are frequently observed in space plasmas.

Key words: plasmas – solar wind – Sun: heliosphere

To Research:
- Tsallis stat mech
- BG statistics

1. INTRODUCTION

Space plasmas from the solar wind to planetary magnetospheres and the outer heliosphere are largely collisionless systems of particles, with long-range interactions, residing in various stationary states out of equilibrium. If a system is in a stationary state, then its recent behavior will continue into the future, namely, the corresponding phase-space probability density is not time dependent over the near future. Consequently, the probability distribution of velocities, of energy, or of particle flux expressed in terms of the energy, is at least temporarily time invariant.

A system whose distribution function of velocities has stabilized to a Maxwellian distribution is in thermal equilibrium. However, this begs the question, what is the correct expression for the probability distribution for systems in stationary states out of equilibrium? Furthermore, space plasmas are rarely Gaussian and instead are frequently characterized by the empirical expression for particle distributions in space plasmas introduced by Vasyliūnas (1968). This is the so-called kappa distribution, parameterized by the index κ ("kappa"). Since then, kappa distributions have been utilized in numerous studies of solar wind (e.g., Chotoo et al. 2000; Mann et al. 2002; Zouganelis et al. 2004; Marsch 2006) and of planetary magnetospheres (e.g., Christon 1987; Mauk et al. 2004; Schippers et al. 2008; Dialynas et al. 2009), as well as in other various plasma-related analyses (e.g., Saito et al. 2000; Raadu & Shafiq 2007; Hellberg et al. 2009).

One great success of Tsallis statistical mechanics is that it offers a concrete statistical foundation for describing stationary states out of equilibrium characterized by kappa distributions, which are the Tsallis statistics analogs of Gaussian distributions in Boltzmann–Gibbs (BG) statistics. Based on a generalization of Boltzmannian entropy and a consistent adaptation of expectation values, the generalization of the Maxwellian distribution of velocities is deduced by extremizing the Tsallis entropy under the constraints of the canonical ensemble. This distribution coincides precisely with the kappa distribution, while the so-called entropic index q (that characterizes the Tsallis entropy) is related to the κ-index of the kappa distribution by $q = 1 + 1/\kappa$.

The Tsallis formalism leads naturally to the exact definition of temperature for stationary states out of equilibrium that is given by the "physical temperature" T_q (Abe 1999; Rama 2000). In the classical BG statistical mechanics, there are three main definitions of temperature: (1) the thermodynamic definition $T_S = (\partial S/\partial U)^{-1}$ (where S and U stand for the classical BG entropy and internal energy, respectively), (2) the kinetic definition, T_K, determined by the second statistical moment of the probability distribution of velocities, and (3) the Lagrangian definition, T, defined by the second Lagrangian multiplier that corresponds to the constraint of internal energy in the canonical ensemble. These three definitions coincide in equilibrium, $T_S = T_K = T$, but they are typically different when the system is out of equilibrium.

Furthermore, in the Tsallis statistical mechanics, the thermodynamic definition of temperature is generalized to the physical temperature, $T_q \equiv (\partial S_q/\partial U_q)^{-1} \cdot [1 + (1 - q) \cdot S_q/k_B]$ (where k_B is the Boltzmann constant), and again, all three definitions coincide in equilibrium, $T_q = T_K = T$. In contrast to the BG formalism, the Tsallis approach maintains the equality $T_q = T_K$, even when the system is in stationary states out of equilibrium. In this way, the kinetic temperature T_K, used in the majority of space plasmas analyses, even in the primary work of Vasyliūnas (1968), is now provided with a solid foundation given by the concept of physical temperature T_q (the thermodynamic definition) and the formalism of Tsallis statistical mechanics (Livadiotis & McComas 2009).

The physical temperature T_q serves the role of the temperature in the modern formalism of non-extensive statistical mechanics. The physical temperature T_q generalizes the zeroth law of thermodynamics (Abe et al. 2001; Wang et al. 2002; Toral 2003). Now, given the equality of T_K, with the physical temperature T_q, all the advantages of a kinetically defined temperature, in contrast to other definitions (Hoover & Hoover 2008), can be ascribed to T_q. After the above clarifications, only one definition of temperature is needed, that of the thermodynamic definition (1) given by the physical temperature T_q, and this is utilized for parameterizing the kappa distributions. Therefore, for the stationary states out of equilibrium and the continuous description of energies, the physical temperature is the actual temperature, and can be used as an independent parameter that labels the distribution (together with the q-index), while the Lagrangian T is just a dependent parameter, $T = T(T_q; q)$.

The Tsallis formalism was first founded simply on the generalization of entropy (Tsallis 1988). However, the thereby extracted canonical probability distribution was problematic because it was not invariant for an arbitrary selection of the ground level of the energy. Subsequently, by considering the so-called escort-expectation values, Beck & Schlogl (1993) and Tsallis et al. (1998) succeeded in recovering this important feature. In this way, the modern Tsallis formalism, widely known as non-extensive statistical mechanism (Tsallis 2009), is based on both the generalizations of entropy and expectation values. While there were several earlier analyses connecting kappa distributions with Tsallis statistical mechanics (e.g., Milovanov & Zelenyi 2000; Leubner 2002; 2004a, 2004b; Yoon et al. 2006, Shizgal 2007; Nieves-Chinchilla & Vinas 2008a, 2008b), all of them were based on the initial Tsallis formalism (or a mixture of the two formalisms) in which the constraints are expressed in terms of the ordinary expectation values, instead of the escort ones (e.g., the constraint of the internal energy in the canonical ensemble). In contrast, Livadiotis & McComas (2009) developed the connection of kappa distribution uniquely with the modern formalism of Tsallis statistical mechanics, in which, among other important consequences, the physical temperature T_q naturally emerges and parameterizes the distribution.

In this paper, we interpret the identity of each stationary state by its specific value of the entropic index q. In general, all the values of the q-index vary continuously, and thus, the spectrum of stationary states is also continuous. We show a novel isothermal procedure that describes the system's transition into different stationary states by varying the q-index. In this way, the variation of temperature is realized under an "iso-metastability" procedure, in which the system is in a fixed stationary state, namely, a state of fixed q-index. From this, we postulate a generalization of the zeroth law of thermodynamics: "Two bodies that are in equilibrium with a third are in equilibrium with each other" in terms of any stationary state: "Two bodies that are in equilibrium *or the same non-equilibrium stationary state* with a third, are in *the same stationary state* with each other."

The Tsallis formalism can be used to develop a measure of the "thermodynamic distance" of stationary states away from equilibrium, which can be expressed in terms of the Tsallis entropic index q. On the other hand, we shall see that for irreversible procedures that increase the entropy of the system, the stationary states gradually evolve toward the specific stationary state at thermal equilibrium. Thus, the further from equilibrium a stationary state is, the more metastable states there are between it and equilibrium. For this reason, we call this measure of "thermodynamic distance" that characterizes stationary states, as q-metastability, denoted by M_q.

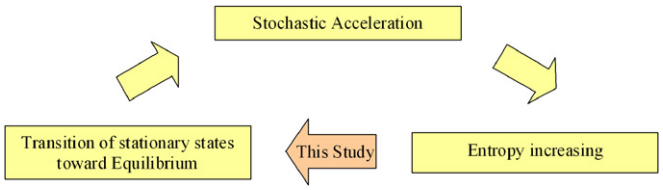

Figure 1. Transition of stationary states toward equilibrium leads to a stochastic acceleration (left arrow). These stochastic acceleration mechanisms are specific diffusion irreversible processes, in which the entropy of the system increases (right arrow). In this study, we complete the cycle by examining how the increasing entropy affects the transition of stationary states.

The stationary states lie in the finite interval between equilibrium ($q = 1$), where we define $M_q \equiv 0\%$, and the furthest possible stationary state from equilibrium ($q \to q_{\rm Max}$), where we define $M_q \equiv 100\%$. We call this non-equilibrium limiting state the "q-frozen state," because it turns out that by approaching this state, the system behaves very much like when the temperature decreases approaching absolute zero. Finally, the values of $q < 1$ also specify stationary states out of equilibrium; however, in this study we primarily focus on values $1 < q < q_{\rm Max}$. The value of $q_{\rm Max}$ depends on the dimensionality of the system, f, i.e., for three-dimensional systems, we have $q_{\rm Max} = \frac{5}{3}$, but regardless of the dimensionality of the system, this maximum value of q-index always represents the q-frozen state.

Note that the system can reach equilibrium, $q = 1$, while it can only approach the q-frozen state, $q \to q_{\rm Max}$. This is the reason we write $q \to q_{\rm Max}$ without using the equality sign. However, a mathematical conflict emerges when we describe equilibrium. The corresponding q-index, $q = 1$, is written in terms of the κ-index as $\kappa = \infty$, instead of the mathematically correct symbolism, $\kappa \to \infty$. The clarification of this is trivial, since the κ-index is dependent on the primary q-index, i.e., $\kappa(q) = 1/(q - 1)$, and thus, $\kappa(q = 1) = \infty$ (note that we are interested in finding the positive values of κ-index). Therefore, with the symbolism of $\kappa = \infty$ (instead of $\kappa \to \infty$), we mean that equilibrium can be reached and not only approached, in contrast to the other extreme of the q-frozen state with the symbolism of $\kappa_{\rm Min} \to \frac{3}{2}$, which can be approached arbitrarily closely but never reached.

By expressing the entropy in terms of the q-index, we show the detailed paths by which the stationary states evolve toward equilibrium. We find that there are two possible solutions for the entropy as a function of q, depending on whether one sets the speed-scale characteristic parameter of the system by relating it to the physical temperature, T_q, or the temperature-like parameter in Tsallis statistics, the Lagrangian, $T = T(T_q; q)$. Here we present both functions and show a number of good reasons to believe that the second interpretation of speed-scale is physically meaningful and can have important implications in at least some physical systems including space plasmas. In either interpretation, the transition of stationary states ultimately tends toward equilibrium and the corresponding stochastic acceleration of particles. In general, the stochastic acceleration mechanisms are specific diffusion irreversible processes, in which the entropy of the system is increasing. In this paper, we focus on how the increasing entropy affects the transition of stationary states, as shown schematically in Figure 1.

The second interpretation implies a specific dynamical scenario of the transition of stationary states toward equilibrium and naturally provides several important values of the κ-index.

Table 1
Critical Indices of Ions, Electrons and Photons in Space Plasmas

Stationary state(s)	Space Plasma	Reference	γ/κ
	Pulsating X-ray source Cygnus X-1	Schreier et al. (1971)	γ, P
q-frozen state	X-rays spectra of accretion disks	Syunyaev et al. (1994); Chakrabarti & Titarchuk (1995)	γ, P
$\kappa_{q-F} \cong 1.5$	Io plasma torus	Steffl et al. (2004)	κ
	Solar wind, inner heliosphere	Fisk & Gloeckler (2006)	γ
	Soft X-rays spectra of Seyfert galaxies	Arnaud et al. (1985)	γ
Fundamental state	Hard X-rays flares	Crosby et al. (1993)	γ
$\kappa_{Fund} \cong 1.63$	Active region transient brightenings	Shimizu (1995)	γ
	Blazar gamma rays	Kifune et al. (1995)	γ
	Soft γ-rays repeater bursts	Göğüş et al. (1999)	γ
	Solar wind, inner heliosheath	Decker et al. (2005)	κ
	Cosmic-ray iron nucleus	Sato et al. (1985)	γ
Escape state	X-rays from accretion disks	Ilovaisky (1986); Miyamoto et al. (1991)	γ
$\kappa_{Esc} \cong 2.45$	Blazar gamma rays	Krennrich et al. (1999); Schroedter et al. (2005); Aharonian et al. (2006)	γ
	Stellar flares	Kashyap et al. (2002)	γ
	Io plasma torus	Steffl et al. (2004)	κ
	Heliospheric tail (ENAs)	McComas et al. (2009)	γ
Far-equilibrium	Blazar γ-rays	Montigny et al. (1995); Venters & Pavlidou (2007)	γ
region,	Solar flares	Aschwanden et al. (2000); Charbonneau et al. (2001); Norman et al. (2001)	γ
$\kappa_{Esc} \geqslant \kappa > \frac{3}{2}$	Interplanetary shocks	Desai et al. (2004)	γ
	CIR's	Mason et al. (2008)	γ
	Quiet times of solar wind, inner heliosphere	Dayeh et al. (2009)	γ
	X-rays from accretion disks	Schreier et al. (1971)	γ
Near-equilibrium	Uranian magnetosphere	Mauk et al. (1987)	γ, P
region,	Solar wind, inner heliosphere	Collier et al. (1996)	κ
$\infty \geqslant \kappa > \kappa_{Esc}$	Possible nanoflares	Benz (2004); Pauluhn & Solanki (2007); Bazarghan et al. (2008)	γ
	Saturnian magnetosphere	Dialynas et al. (2009)	κ

Notes.
γ: A power law was fitted and the spectral index refers to the H-E region.
κ: A kappa distribution was fitted (either first or second kind (Livadiotis & McComas 2009)).
P: Possible coexistence of more than one stationary state. The steeper law reveals in law energies while the flatter law dominates in high energies (see the text).

Interestingly, these values have also been frequently observed in space plasmas: (1) $\kappa_{EQ} = \infty$ (e.g., Hammond et al. 1996), corresponding to the specific stationary state at equilibrium; (2) $\kappa_{q-F} \cong 1.5$, which seems to act as an attractor of states, corresponding to the q-frozen state; (3) $\kappa_{Fund} \cong 1.63$, detected in inner heliosheath, beyond the termination shock; and (4) $\kappa_{Esc} \cong 2.45$ that has the unique role of separating the stationary states near equilibrium, with $\kappa > \kappa_{Esc}$, from those near the q-frozen state, with $\kappa_{Esc} \geqslant \kappa$. (For the references on these critical κ-indices of stationary states out of equilibrium, see Table 1 and Section 4.3).

The paper is organized as follows. In Section 2, we discuss the permissible values of the kappa indices. These are extracted from the convergence of the integral that gives the second statistical moment and depends on the dimensionality of the system. In Section 3, we examine the furthest possible stationary state from equilibrium, the q-frozen state. In Section 4, we develop the measure of the "thermodynamic distance" of stationary states from equilibrium, called q-metastability, which fulfills specific conditions and is expressed in terms of the Tsallis entropic index q. We demonstrate its role in the spectrum-like arrangement of stationary states. We also show how the q-metastability measure characterizes the identity of each stationary state. With the help of this q-metastability measure, we characterize the various stationary states that have been detected by the observations of the solar wind, planetary, or other space plasmas. In Section 5, we construct the Tsallis entropy and its expression in terms of the q-index and present how the spontaneous entropic procedures affect the values of q-index and the transition of stationary states. In Section 6, we deal with the dynamics of stationary state transitions and show the detailed paths by which the transition of stationary states evolves toward equilibrium. Finally, Section 7 summarizes the primary results of this study and provides some conclusions.

2. THE MARGINAL STATIONARY STATES

The permissible values of the kappa indices are determined from the requirements that the integrals of normalization, mean value, and second statistical moment converge. The latter implies stronger conditions; hence, the following integral must have a finite value:

$$\int_0^\infty w^2 \cdot P(w; \theta_{\rm eff}; \kappa) g_{\rm V}(w) dw < +\infty, \quad (1)$$

where the (spherically symmetric) kappa distribution

$$P(w; \theta_{\rm eff}; \kappa) \sim \left[1 + \frac{1}{\kappa - \frac{f}{2}} \cdot \left(\frac{w}{\theta_{\rm eff}}\right)^2\right]^{-\kappa-1}, \quad (2)$$

and the density of velocity states,

$$g_{\rm V}(w) \sim w^{f-1}, \quad (3)$$

stand for an f-dimensional space of velocities. We defined $\vec{w} \equiv \vec{u} - \vec{u}_b$, that is the particle velocity measured in the reference frame of the plasma's bulk flow; $\vec{u}$ and $\vec{u}_b$ stand for the particle

and bulk flow velocities, measured in the observing spacecraft's reference frame. The speed-scale parameter $\theta_{\rm eff}$ is connected with the physical temperature, namely, $\theta_{\rm eff} \equiv \sqrt{2k_B T_q/\mu}$, where μ is the particle mass. Its role is simply to express the temperature of the system (T_q) in velocity dimensions.

In the classical case of the stationary state at equilibrium, i.e., $\kappa = \infty$ (or $q = 1$), the probability distribution is given by a Maxwellian, which decays exponentially, and thus, the relevant integrals converge for any power-like expression of the density of velocity states, $g_{\rm V}(u)$. However, in the case of the power-law-like decay of the kappa distribution (for $\kappa < +\infty$), the convergence is not trivial, as it depends on the value of the κ-index and the dimensionality f. In particular, the integrals converge as soon as the relevant integrants in the high-energy limit of $w \to \infty$ attain at least a power-law decay of $1/w^r$, with $r > 1$ (Ferri et al. 2005). At this limit, the kappa distribution (2) has the asymptotic behavior of $P(w;\theta_{\rm eff};\kappa) \sim w^{-2(\kappa+1)}$, so that

$$w^2 \cdot P(w;\theta_{\rm eff};\kappa) g_{\rm V}(w) \sim w^{-2\kappa+f-1} \Rightarrow 1 < r = 2\kappa - f + 1. \quad (4)$$

Hence, in order for the integral of the second statistical moment to converge, we obtain the condition

$$\kappa > \frac{f}{2}, \quad \text{or } q < \frac{f+2}{f}, \quad (5)$$

(where we utilized $q = 1 + 1/\kappa$). The requirement of (5) is general for any f-dimensional system. For the three-dimensional case that characterizes space plasmas amongst many other systems, we obtain

$$\kappa > \frac{3}{2}, \quad \text{or } q < \frac{5}{3}, \quad (6)$$

and thus, all stationary states that can be detectable within the framework of Tsallis statistical mechanics must have values of the κ-index within the interval $\kappa \in (\frac{3}{2}, \infty]$, or, values of the q-index within the interval $q \in [1, \frac{5}{3})$. The first boundary value, i.e., $\kappa = \infty$ (or $q = 1$), defines equilibrium, while the second boundary value, i.e., $\kappa \to \frac{3}{2}$ (or $q \to \frac{5}{3}$), gives the furthest stationary state from equilibrium that can be approached. All the attainable stationary states lie between these extreme states.

3. FURTHEST FROM EQUILIBRIUM: THE q-FROZEN STATIONARY STATE

In this section, we focus on the concept of the stationary state furthest from equilibrium, the q-frozen state, in three-dimensional systems; however, generalization to other dimensions, f, is straightforward, following a parallel development. We have seen that for a three-dimensional system, the permissible (positive) values of κ-index span the interval $\kappa \in (\frac{3}{2}, \infty]$, or equivalently, $q \in [1, \frac{5}{3})$. Let us now focus on the two extreme stationary states. The marginal value of $\kappa = \infty$ (or $q = 1$) is the best-known stationary state at equilibrium that has been already widely studied within the framework of BG statistical mechanics, and its Maxwellian distribution of velocities is observed across a wide variety of physics, including some space plasmas (e.g., Hammond et al. 1996).

In contrast to equilibrium, which is trivially achievable, the other extreme stationary state of $\kappa \to \frac{3}{2}$ (or $q \to \frac{5}{3}$) is not attainable, even though it can be approached arbitrarily closely. In Figure 2(a), we depict the kappa distribution $P(w;\theta_{\rm eff};\kappa)$ in terms of the velocity $w \equiv |\vec{u} - \vec{u}_b|$ for various values of

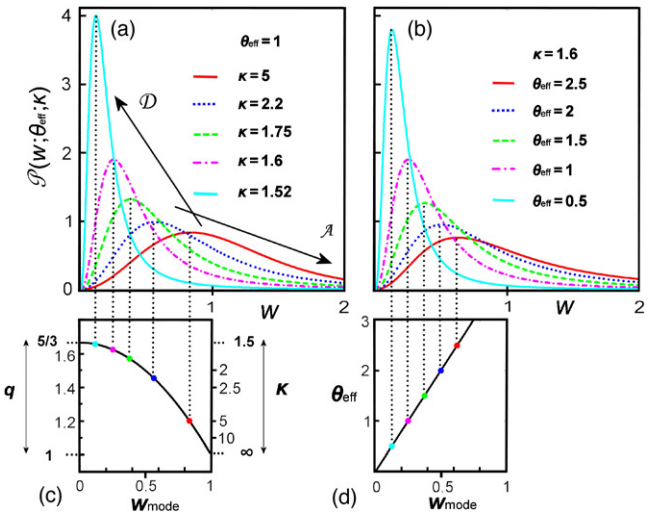

Figure 2. Kappa distribution is depicted for (a) constant temperature $\theta_{\rm eff} = 1$ and various values of the κ-index (isothermal procedure: fixed temperature T_q or $\theta_{\rm eff}$); and for (b) a constant index $\kappa = 1.6$ and various values of temperature $\theta_{\rm eff}$ (iso-metastability procedure: fixed value of the κ-index). In the former case, by decreasing κ, the distribution is shifted to smaller velocities (or energies) toward the q-frozen state, causing a phenomenological deceleration (along the indicated D array). By increasing κ, the distribution is shifted to larger velocities toward equilibrium (along the indicated A array). In the latter case, the distribution is shifted to smaller (or larger) velocities due to the more familiar procedure of decreasing (or increasing) the temperature and staying at the same stationary state. The shifting of distributions is also demonstrated by depicting the most possible velocity $w_{\rm mode}(\theta_{\rm eff};\kappa)$: (c) For constant temperature, $\theta_{\rm eff} = 1$, and various values of κ-index; and (d) for constant index $\kappa = 1.6$ and various values of $\theta_{\rm eff}$.

the κ-index (and $\theta_{\rm eff} = 1$), showing the statistical behavior of the particles, as the extreme stationary state of $\kappa \to \frac{3}{2}$ is approached. The distribution is normalized by the density of velocity states $g_{\rm V}(w) = 4\pi w^2$, namely, $\int_0^\infty P(w;\theta_{\rm eff};\kappa)dw = 1$, with the whole distribution $P(w;\theta_{\rm eff};\kappa) \equiv P(w;\theta_{\rm eff};\kappa) g_{\rm V}(w)$ to be given by

$$P(w;\theta_{\rm eff};\kappa) = \frac{4}{\sqrt{\pi}} \cdot \frac{\left(\kappa - \frac{3}{2}\right)^{-\frac{3}{2}} \Gamma(\kappa+1)}{\Gamma\left(\kappa - \frac{1}{2}\right)} \cdot \theta_{\rm eff}^{-3} \cdot \left[1 + \frac{1}{\kappa - \frac{3}{2}} \cdot \left(\frac{w}{\theta_{\rm eff}}\right)^2\right]^{-\kappa-1} \cdot w^2. \quad (7)$$

The mode of the distribution can be easily found to be given by the most possible velocity

$$w_{\rm mode}(\theta_{\rm eff};\kappa) = \sqrt{\frac{\kappa - \frac{3}{2}}{\kappa}} \cdot \theta_{\rm eff}, \quad (8)$$

attaining the maximum of the probability density, i.e.,

$$P_{\rm mode}(\theta_{\rm eff};\kappa) = \frac{4}{\sqrt{\pi}} \cdot \frac{1}{\sqrt{\kappa - \frac{3}{2}} \cdot \theta_{\rm eff}} \cdot \frac{\Gamma(\kappa)}{\Gamma(\kappa - \frac{1}{2})} \cdot \left(\frac{\kappa}{\kappa+1}\right)^{\kappa+1}. \quad (9)$$

Note that $w_{\rm mode}$ is proportional to $\theta_{\rm eff}$, but depends also on the values of the κ-index. For any value of κ, it is always restricted to the interval $0 < w_{\rm mode} \leqslant \theta_{\rm eff}$, with the equality applying only at equilibrium ($\kappa \to \infty$). For smaller values of κ, the maximum $w_{\rm mode}$ is also smaller and shifted closer to zero. The suprathermal tails appear sufficiently far from this maximum, $w > w_{\rm mode}$, and for lower values of $w_{\rm mode}$ the tail is expected to become

more dominant. This is consistent with Equation (8), where with decreasing kappa values, $w_{\rm mode}$ also decreases, generating suprathermal tails in the distribution.

Figure 2(a) shows that as the κ-index increases (or the q-index decreases) and the stationary state becomes closer to equilibrium, the probability distribution (7) is shifted to larger values of velocity. This can also be shown through the most likely velocity $w_{\rm mode}(\theta_{\rm eff};\kappa)$, which is depicted in Figure 2(c), respectively, for the same values of the κ-index (and $\theta_{\rm eff}=1$). If the system attains stationary states of larger values of the κ-index, then the system's particles are characterized by larger values of velocities (or energies). Thus, a phenomenological acceleration is caused. The relevant procedure of the transition of the system through various metastable stationary states of larger values of the κ-index toward equilibrium (indicated in Figure 2(a) by an "A") is called stochastic acceleration. The opposite procedure in which the transient metastable stationary states attain smaller values of the κ-index and the system's particles depart to smaller velocities (or energies) is also very interesting. Here, a phenomenological deceleration is caused (indicated in Figure 2(a) by a "D"), and the system is driven away from equilibrium toward the other extreme stationary state of $\kappa\to\frac{3}{2}$, or $q\to\frac{5}{3}$.

The probability distributions for the two extreme stationary states are written as follows.

1. The stationary state at equilibrium ($\kappa=\infty$): the probability distribution is Maxwellian, $P(w;\theta_{\rm eff};\kappa=\infty)\cong\pi^{-\frac{3}{2}}\cdot\theta_{\rm eff}^{-3}\cdot e^{-(w/\theta_{\rm eff})^2}$, and by setting $P_{\rm EQ}(w;\theta_{\rm eff})\equiv P(w;\theta_{\rm eff};\kappa=\infty)$ (where the notation "EQ" stands for the stationary state in equilibrium), we have

$$P_{\rm EQ}(w;\theta_{\rm eff})\cong\frac{4}{\sqrt{\pi}}\cdot\theta_{\rm eff}^{-3}\cdot e^{-(w/\theta_{\rm eff})^2}\cdot w^2. \qquad (10)$$

2. The stationary state furthest from equilibrium: $\kappa\to\frac{3}{2}$, or $\kappa\cong\frac{3}{2}+\delta+O(\delta^2)$, we have $P(w;\theta_{\rm eff};\delta)\cong 3(4\pi)^{-1}\cdot\delta\cdot\theta_{\rm eff}^{2+2\delta}\cdot w^{-5-2\delta}$, which is an approximation $\forall w\gg\sqrt{\delta}\cdot\theta_{\rm eff}>0$. Hence, the whole distribution $P_{\rm q-F}(w;\theta_{\rm eff};\delta)=P(w;\theta_{\rm eff};\delta)g_{\rm V}(w)$ (where the notation "q-F" stands for the "q-frozen" stationary state as we shall see directly below), is given by

$$P_{\rm q-F}(w;\theta_{\rm eff};\delta)\cong 3\cdot\delta\cdot\theta_{\rm eff}^2\cdot w^{-3},\quad \forall\ w\gg\sqrt{\delta}\cdot\theta_{\rm eff}>0. \qquad (11)$$

On the other hand, $\forall\ w\ll\sqrt{\delta}\cdot\theta_{\rm eff}$, a different approximation is produced,

$$P_{\rm q-F}(w;\theta_{\rm eff};\delta)\cong 3\cdot\delta^{-\frac{3}{2}}\cdot\theta_{\rm eff}^{-3}\cdot w^2,\forall\ w\ll\sqrt{\delta}\cdot\theta_{\rm eff}>0. \qquad (12)$$

We note that the intervals $0\leqslant w\leqslant w_{\delta,1}$ and $w_{\delta,2}\leqslant w<+\infty$, with $w_{\delta,1}=\sqrt{\delta}\cdot\theta_{\rm eff}$, $w_{\delta,2}=\sqrt{\frac{3}{2}}\sqrt{\delta}\cdot\theta_{\rm eff}$, normalize $P_{\rm q-F}(w;\theta_{\rm eff};\delta)$ as given in Equations (12) and (11), respectively. The values $w_{\delta,1}$ and $w_{\delta,2}$ are quite close to the mode $w_{\rm mode}(\theta_{\rm eff};\delta)$, which, for $\delta\ll 1$, is approximated as

$$w_{\rm mode}(\theta_{\rm eff};\delta)\cong\sqrt{\frac{2}{3}}\sqrt{\delta}\cdot\theta_{\rm eff}, \qquad (13)$$

while the relevant maximum of the probability density is

$$P_{\rm mode}(\theta_{\rm eff};\delta)\cong 2\left(\frac{3}{5}\right)^{\frac{5}{2}}\cdot\frac{1}{\sqrt{\delta}\cdot\theta_{\rm eff}}, \qquad (14)$$

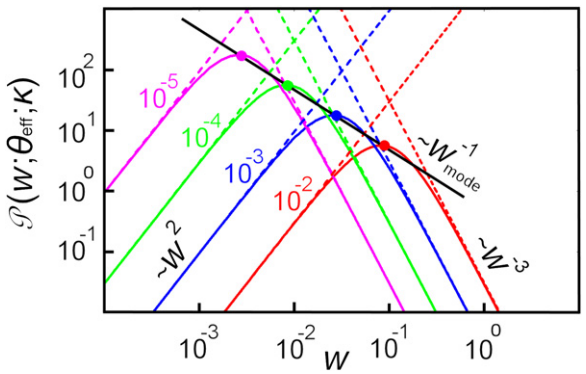

Figure 3. Probability distribution (Equation 7) is depicted on a log–log scale for values of the κ-index close to $\kappa\to\frac{3}{2}$, i.e., $\delta=10^{-2}$, 10^{-3}, 10^{-4}, 10^{-5} ($\kappa\equiv\frac{3}{2}+\delta$). We verify the approximations (Equations (11), (12) and (15)).

(Equations (13) and (14) are approximations of Equations (10) and (11) for $\kappa\cong\frac{3}{2}+\delta+O(\delta^2)$). Then, we easily find that $w_{\delta,1}=\sqrt{\frac{3}{2}}\cdot w_{\rm mode}$, $w_{\delta,2}=\frac{3}{2}\cdot w_{\rm mode}$. In Figure 3, the probability distribution, Equation (7), is depicted for various values of the κ-index as $\kappa\to\frac{3}{2}$, where we verify the approximations given in Equations (11) and (12). Hence, the mode plays the role of the boundary between these two functional behaviors of $P_{\rm q-F}(w;\theta_{\rm eff};\delta)$. In addition, we note that

$$w_{\rm mode}(\theta_{\rm eff};\delta)\cdot P_{\rm mode}(\theta_{\rm eff};\delta)\cong\frac{36}{25\sqrt{10}}\cong 0.455. \qquad (15)$$

Namely, for any value of κ-index being arbitrary close to $\kappa\to\frac{3}{2}$ (that is for any small value of δ), the product of the maximum probability density with the relevant velocity is independent of κ-index, which has the constant value $\cong$0.455. Figure 3 shows that the geometrical locus of all the modes (black solid line) is given by the function $P_{\rm mode}(w)\cong 0.455/w$, verifying Equation (15).

The above considerations support the fact that for any small value of δ, the probability distribution of velocities $P_{\rm q-F}(w;\theta_{\rm eff};\delta)$ will never be equal to zero for non-zero velocities, since its unimodal structure is always preserved. In other words, the most probable velocity will be given by the non-zero velocity at the mode, i.e., $w_{\rm mode}(\theta_{\rm eff};\delta)\neq 0$, and thus, the particles never slow down to exactly zero velocity in this statistical mechanics treatment.

It is clear that the marginal probability distribution of $\kappa\to\frac{3}{2}$ (or $q\to\frac{5}{3}$) cannot be reached, in a very similar way to how absolute zero temperature $\theta_{\rm eff}\to 0$ can only be approached, but is ultimately unattainable for any stationary state, even for the classical Maxwellian in equilibrium. In fact, it is remarkable that the behavior of approaching both the limits, $\theta_{\rm eff}\to 0$ or $\kappa\to\frac{3}{2}$, is so qualitatively similar. Indeed, the probability distribution, Equation (9), can be written as

$$P(w;\theta_\kappa;\kappa)=\frac{4}{\sqrt{\pi}}\cdot\frac{\kappa^{-\frac{1}{2}}\Gamma(\kappa)}{\Gamma(\kappa-\frac{1}{2})}\cdot\theta_\kappa^{-3}\cdot\left[1+\frac{1}{\kappa}\left(\frac{w}{\theta_\kappa}\right)^2\right]^{-\kappa-1}\cdot w^2, \qquad (16)$$

where we define $\theta_\kappa\equiv\sqrt{(\kappa-\frac{3}{2})/\kappa}\cdot\theta_{\rm eff}$, so that both the limits of $\kappa\to\frac{3}{2}$ or $\theta_{\rm eff}\to 0$ can be described by the same single limit, that is $\theta_\kappa\to 0$. Then, the relevant probability distribution can

be approximated by

$$P_{\mathrm{q-F}}(w;\theta_\kappa) \cong \frac{9}{2}\cdot\theta_\kappa^2\cdot w^{-3}, \quad (17)$$

that is rewriting Equation (11), given the definition of θ_κ.

Therefore, a phenomenological deceleration of the particles can be realized by decreasing either the value of the κ-index, or the characteristic speed-scale parameter θ_{eff} (i.e., the temperature T_q). Both the procedures can be represented by the unified scheme of $\theta_\kappa \to 0$. Since we are unfamiliar with the physical meaning of having $\theta_\kappa \to 0$ by decreasing the κ-index, let us focus first on the other case, of $\theta_\kappa \to 0$ by decreasing the temperature. In Figure 2(b), we depict the probability distribution (7) for $\kappa = 1.6$ and various values of θ_{eff}, while in Figure 2(d), we show the most likely velocity $w_{\mathrm{mode}}(\theta_{\mathrm{eff}};\kappa)$, respectively, for the same values of θ_{eff} (and $\kappa = 1.6$). As θ_{eff} (or T_q) increases, the distribution, Equation (7), is shifted to larger values of velocity producing a phenomenological acceleration of the particles, while for θ_{eff} (or T_q) decreasing, the distribution, Equation (7), is shifted to smaller values of velocity, and a phenomenological deceleration of the particles is observed.

If the system of particles is freezing by decreasing the temperature, $\theta_{\mathrm{eff}} \to 0$ (or $T_q \to 0$), then it is reasonable to say that a new kind of freezing can be defined by decreasing the κ-index (or, by increasing the q-index) and attaining the furthest stationary state from equilibrium, that is of $\kappa \to \frac{3}{2}$ (or $q \to \frac{5}{3}$). This is the reason we call the extreme stationary state furthest from equilibrium, a "frozen" state. Specifically, we call it the "q-frozen" stationary state, in order to underline the fact that the freezing procedure is not being reached by the familiar method of decreasing temperature, but by the quite unfamiliar process of maximizing the distance from equilibrium by decreasing the κ-index (or, by increasing the q-index).

Finally, we stress that approaching the q-frozen stationary state is a procedure in which the κ-index (or q-index) changes, while the physical temperature T_q (or θ_{eff}) remains invariant under this transition into different stationary states. The fact that the value of temperature T_q is invariant under the decreasing of the κ-index as the system approaches the q-frozen state ensures that this new and extraordinary procedure of freezing is not inconsistent with the third law of thermodynamics, which only concerns the limit of $T_q \to 0$ (or $\theta_{\mathrm{eff}} \to 0$). We remark that in each transition, either from the q-frozen state toward equilibrium, or vice versa, both phenomenological acceleration and deceleration procedures take place at the same time. This is because the particle distributions with larger peaks at lower energies (decelerated) also have higher tails at high energies (accelerated). Even though both processes occur simultaneously, the vast majority of the particles move toward the deceleration side when approaching the q-frozen state. In this case, the deceleration is dominant, while the opposite procedure of acceleration is dominant for transitions toward equilibrium.

4. A MEASURE OF THE DEPARTURE FROM EQUILIBRIUM

4.1. The Spectrum-Like Arrangement of Stationary States

The previous analysis showed that stationary states can be arranged according to the values of the q-index (or κ-index), so that the larger the value of the q-index (or the smaller the value of the κ-index) is, the further from equilibrium and the closer to the q-frozen stationary state the system is. As $q \to \frac{5}{3}$ (or $\kappa \to \frac{3}{2}$), the q-frozen state is attained, and thus, this state is the furthest possible stationary state from equilibrium. Therefore, the whole set of different stationary states can be realized in a spectrum-like arrangement of different values of the q-index (or the κ-index) in the interval $q \in [1, \frac{5}{3})$ (or $\kappa \in (\frac{3}{2}, \infty]$).

Clearly, the characteristic values of the κ-index, or equivalently of the q-index, can provide a measure of the departure of the stationary states from equilibrium (e.g., Burlaga & Viñas 2005). Indeed, in this section, we express this "thermodynamic distance" of stationary states from equilibrium as a function of the q-index. Firstly, we have to show that both the extreme stationary states, equilibrium and the q-frozen state, have characteristic universalities.

The universal behavior of the specific stationary state at equilibrium is trivial. Indeed, independently of the dimensionality f of the system, this will be always attained for $q = 1$ ($\kappa = \infty$), while the characteristic probability distribution of velocities will be a Maxwellian $P_{\mathrm{EQ}}(w;\theta_{\mathrm{eff}}) \sim e^{-(w/\theta_{\mathrm{eff}})^2}$. Further, it is not so trivial to define the universality of the other extreme—the q-frozen state. This is because the maximum value of the q-index (or the minimum value of the κ-index) that leads to the q-frozen state is always dependent on the dimensionality of the system. For $\kappa \cong \frac{f}{2} + \delta + O(\delta^2)$, we have $P(w;\theta_{\mathrm{eff}};\delta) \sim w^{-f-2-2\delta}$, ($\forall w \gg \sqrt{\delta}\cdot\theta_{\mathrm{eff}} > 0$). Then, because of $g_{\mathrm{V}}(w) \sim w^{f-1}$ (3), we find that the whole distribution is $P_{\mathrm{q-F}}(w;\theta_{\mathrm{eff}};\delta) \sim w^{-f-2-2\delta}\cdot w^{f-1} = w^{-3-2\delta} \cong w^{-3}$, independently of the dimensionality f. Therefore, the probability distribution that characterizes the q-frozen stationary state has a universal functional behavior, i.e., the power law of $P_{\mathrm{q-F}}(w;\theta_{\mathrm{eff}}) \sim w^{-3}$.

This universal behavior leads us to ascribe a fixed "thermodynamic distance" between the q-frozen state and equilibrium. In addition, the q-frozen state is the furthest stationary state from equilibrium, while all the other stationary states must lie between. Hence, the maximum "thermodynamic distance" is fixed, while each stationary state represents only a specific fraction of this total distance. In this way, the q-frozen state can be referred to as 100% away from equilibrium, while all the stationary states lie between the extreme stationary states of 0% (equilibrium) and 100% (q-frozen state).

4.2. Definition of the q-metastability Measure

It should now be clear that for systems of different dimensionality, values of the q-index, e.g., $q = \frac{5}{3}$ (or $\kappa = \frac{3}{2}$), do not characterize the same stationary state. Indeed, for $f = 3$, the value $q = \frac{5}{3}$ stands for the q-frozen state that is 100% away from equilibrium. But for $f = 1$, the value $q = \frac{5}{3}$ is just a stationary state within the interval [0% − 100%), since the q-frozen state is now given by $q = 3$ (or $\kappa = \frac{1}{2}$). Hence, the q-index by itself does not provide a measure of how far various stationary states are from equilibrium. The same clearly holds for the κ-index, although the q-index is more fundamental than the κ-index, since it originates directly from basic concepts of the Tsallis statistical mechanics, such as the generalized entropy and the escort expectation value (see Tsallis 1988; Tsallis et al. 1998). In the following, we develop a measure of the "thermodynamic distance" of stationary states from equilibrium, which is given by a simple expression of q- or κ-index and is mathematically well founded.

All the stationary states that are described by the Tsallis entropy maximization and the derived kappa distribution can be considered as metastable states that transit under certain

procedures toward equilibrium (Section 6). For this reason, we call the "thermodynamic distance" of each stationary state from equilibrium, the "q-metastability measure," M_q. This measure has to be a function of both the q-index and its maximum value that corresponds to the q-frozen state $q_{\rm Max}$, i.e., $M_q = M_q(q; q_{\rm Max})$. Further, all possible values must be $0\% \leqslant M_q(q \geqslant 1; q_{\rm Max}) < 100\%$.

Since equilibrium is described by the classical limit of $q \to 1$, then it is required that $M_q(1; q_{\rm Max}) = 0$. On the other hand, its largest value is attained for the q-frozen stationary state, so that $M_q(q_{\rm Max}; q_{\rm Max}) = 1$. As $q \geqslant 1$ increases, the system shifts further from equilibrium. Thus, the function $M_q(q; q_{\rm Max})$ has to be monotonically increasing with q, i.e., $\partial M_q(q; q_{\rm Max})/\partial q > 0$. In addition, we adopt the property $M_q(1/q; q_{\rm Max}) = -M_q(q; q_{\rm Max})$ as suggested by the duality of the ordinary-escort probabilities. In particular, the ordinary (discrete) probability distribution $\{p_k\}_{k=1}^{W}$ leads to the escort one $\{P_k\}_{k=1}^{W}$, after the transformation $P_k \sim p_k^q$ applies, while the inverse transformation is characterized by the inverse index, i.e., $p_k \sim P_k^{1/q}$ (Beck & Schlogl 1993). In this way, we have $q_{\rm Min} = 1/q_{\rm Max}$, and $M_q(1/q_{\rm Max}; q_{\rm Max}) = -1$. One simple function that has all the properties needed for $M_q(q; q_{\rm Max})$ is

$$M_q\left(q; q_{\rm Max} = \frac{f+2}{f}\right) = (f+1)\cdot\frac{q-1}{q+1}, \text{ or for } f = 3,$$
$$M_q\left(q; q_{\rm Max} = \frac{5}{3}\right) = 4\cdot\frac{q-1}{q+1}. \quad (18)$$

4.3. Interpreting the Observations

Having constructed a simple mathematical tool for describing the deviation of stationary states from equilibrium, it is straightforward to characterize the stationary states that have been detected by various observations.

The q-frozen stationary state was first detected in space particle populations by Steffl et al. (2004) in the Io plasma torus. In particular, by analyzing the data from UVIS onboard the Cassini spacecraft, they found that the derived value of the kappa index that describes ions and electrons has a value around $\kappa \sim 5$ for the inner layers of $\sim 6\, R_{\rm Io}$ (Io's radius) and decreased with the radial distance reaching asymptotically the q-frozen value $\kappa_{\rm q-F} \cong 1.5$ for $\sim 9\, R_{\rm Io}$. The q-frozen state was also detected in the solar wind protons by Fisk & Gloeckler (2006). This analysis was based on the observations of *Ulysses* and *Advance Composition Explorer* (*ACE*), Solar Wind Ion Composition Spectrometers (SWICS) that collected data on the suprathermal tails at distances ranging from 1 AU to 5.4 AU. In particular, by plotting the probability distribution of velocities, $p(u)$, so that the contribution of the density states of velocities, $g_{\rm V}(u) \sim u^2$, to be excluded, they concluded that there is a "universal" power law in the high-energy (H-E) region, $p_{\rm H-E}(u) \sim u^{-5}$. Therefore, the whole distribution, that is when the density states of velocities are restored, is characterized by the power law of $P_{\rm H-E}(u) \equiv p_{\rm H-E}(u) g_{\rm V}(u) \sim u^{-3}$. Note that this can be written also as $P_{\rm H-E}(w) \sim w^{-3}$ (since for the H-E region $w \equiv |\vec{u} - \vec{u}_b| \cong u$). This is the probability distribution that characterizes the q-frozen stationary state (see Equation (11)), having the indices $\kappa \to \kappa_{\rm Min} = \frac{3}{2}$, $q \to q_{\rm Max} = \frac{5}{3}$, and q-metastability measure $M_q = 100\%$.

Close to the marginally valid value of $\kappa \cong 1.5$ is the value of the κ-index estimated by the analysis of Decker et al. (2005), that is $\kappa \cong 1.63$. This analysis was based on recent observations from the *Voyager 1* Low Energy Charged Particle (LECP) detector that collected data in the inner heliosheath, the distant solar wind beyond the termination shock. In particular, by plotting the flux of particles versus energies, Decker et al. (2005) detected a power-law suprathermal ($u \gg u_b$) tail for protons with a spectral index of about $\gamma \cong 1.6$, while the precise value of $\kappa \cong 1.63$ was estimated by the fitting of a kappa distribution. This value of the κ-index was subsequently used by other authors in several theoretical analyses and models (e.g., Prested et al. 2008; Heerikhuisen et al. 2008; Schwadron et al. 2009).

For the value of $\kappa \cong 1.63$, we find a deviation $M_q \cong 93.8\%$ away from equilibrium, which verifies that the stationary state detected by Decker et al. (2005) is indeed close to the q-frozen state. But still, the difference of the observed values $\kappa \cong 1.5$ and $\kappa \cong 1.63$ is not negligible, and this difference needs to be examined and understood. In Section 5.1, we provide a detailed interpretation. In particular, we show that the q-frozen stationary state results from the gradual augmentations of entropy under arbitrary internal irreversible procedures that might take place in the solar wind (or other space plasmas). On the other hand, the specific stationary state that was detected by Decker et al. (2005) is the one that minimizes the entropy, so that any external mechanism that can decrease the entropy leads to the stationary state of $\kappa \cong 1.63$. Such a mechanism is the rejuvenation of entropy potentially caused by the pick-up ions, which we discuss in Section 5.2.

The state of $\kappa_{\rm Esc} \cong 2.45$ was first detected in space particles populations (Mauk et al. 1987) in the Uranian magnetosphere. The spectral indices in the H-E region were found to be distributed in the near-equilibrium region, $\infty \geqslant \kappa > \kappa_{\rm Esc}$. Similar results were found by Dialynas et al. (2009), by examining particle distributions in the Saturnian magnetosphere from the Magnetospheric Imaging Instrument (MIMI) suite onboard *Cassini* (see also Dialynas et al. 2008). They estimated the values of the κ-index for a large number of probability distributions (both protons and O^+), that were organized by the L-shell of Saturn over 5–20 Saturnian radii. The estimated values of the κ-index were found to be large and distributed in a remarkable arrangement (compare Figure 2 in Dialynas et al. 2009), ranging mostly between 2–2.5 and 11–13, corresponding to deviation measure values ranging between 15%–20% and 65%–80%. The histograms of the κ-index values are shown in the insets of Figures 4(b) and (d), respectively, for the hydrogen and oxygen cations, where we observe that the most probable values are $\kappa_{\rm H^+} \cong 3.5$ and $\kappa_{\rm O^+} \cong 5$, corresponding to measure values $M_{q,\rm H^+} \cong 50\%$ and $M_{q,\rm O^+} \cong 35\%$.

It is fascinating that the solar wind hydrogen ions are characterized by large deviations from equilibrium, $\kappa < 2.45$ or $M_q > 67.8\%$ (see the work of Dayeh et al. 2009 below), while the ions in the Saturnian magnetosphere were found to be characterized by significantly smaller deviations, that is of $\kappa > 2.45$ or $M_q < 67.8\%$. This fact clearly supports the idea that the Saturnian magnetospheric plasma is approaching a quasi-equilibrium status, namely, stationary states near equilibrium. In contrast to the sparse heliosphere, the dense hydrogen and oxygen in the Saturnian magnetosphere produces copious charge exchange between hydrogen ions and oxygen neutral atoms (and vice versa, $H^+ + O \rightleftarrows H + O^+$). This interaction leads the hydrogen ions to distribute in a specific way, inheriting the respective characteristics of oxygen ions, such as the same κ-index. Interestingly, the protons were found to have spectral indices similar to that of O^+, but still, a significant difference

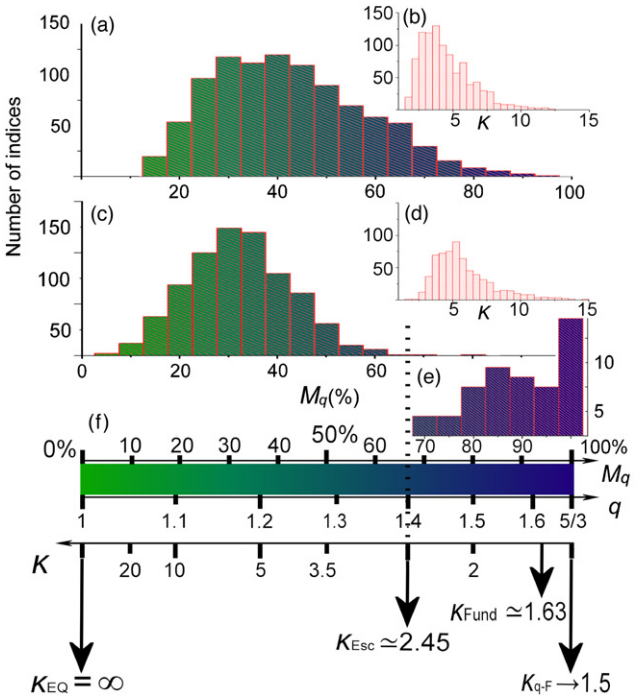

Figure 4. Histograms of the κ-indices of the near equilibrium stationary states as detected by Dialynas et al. (2009) for the protons (b) and oxygen cations (d) in the Saturnian magnetosphere. The protons have spectral indices similar to that of O^+, but still, a significant difference exists between the most probable values of $\kappa_{H^+} \cong 3.5$ and $\kappa_{O^+} \cong 5$ that clearly implies $M_{q,H^+} \neq M_{q,O^+}$. This difference is recovered when we plot directly the respective histograms (a) and (c) of the q-metastability measure, where the most probable values are $M_{q,H^+} \cong 40\%$ and $M_{q,O^+} \cong 35\%$. In panel (e), we depict the histogram of the q-metastability values of the indices of the far equilibrium (or near q-frozen state) stationary states as detected by Dayeh et al. (2009) for the inner heliosphere. Finally, the critical values of the κ-index characterizing equilibrium $\kappa_{EQ} = \infty$, the escape state $\kappa_{Esc} \cong 2.45$, the fundamental state $\kappa_{Fund} \cong 1.63$, and the q-frozen state $\kappa_{q-F} \cong 1.5$, are indicated in the whole interval $\kappa \in (\frac{3}{2}, \infty]$ (or $q \in [1, \frac{5}{3})$, $M_q \in [0\%, 100\%)$) in panel (f).

exists between the values of $\kappa_{H^+} \cong 3.5$ and $\kappa_{O^+} \cong 5$ that clearly implies $M_{q,H^+} \neq M_{q,O^+}$. Surprisingly, this difference is recovered when we plot directly the histograms of the q-metastability measure. In this case, we observe in Figures 4(a) and (c) that the most probable values are $M_{q,H^+} \cong 40\%$ and $M_{q,O^+} \cong 35\%$. Given that the bin length in the histograms is $\delta M_q \cong 5\%$, then $M_{q,H^+} \cong M_{q,O^+}$.

Therefore, the observed arrangement of stationary states near equilibrium is quite similar for both protons and O^+. In particular, around ~99.5% of the values of oxygen κ-indices were found to be distributed in the interval $\kappa > 2.45$. The same arrangement seems to be followed by the protons, since ~90% of the relevant values of κ-indices are distributed in the same interval. The existence of ~10% of κ-indices having values $\kappa < 2.45$ might be due to Saturnian pick-up ions and/or solar wind protons, which have large values of M_q, and are also present in the Saturnian magnetosphere.

Clearly, stationary states near equilibrium are also detected in solar wind, (e.g., Hammond et al. 1996). However, these appear to be rather rare. For instance, the work of Dayeh et al. (2009) showed that all the estimated κ-indices were arranged in the interval $\kappa < 2.45$. In this work, Dayeh et al. (2009) estimated directly the spectral index in the suprathermal tail spectra of the heavy ions CNO, Ne-S, and Fe during 1 AU quiet times of solar cycle 23 (from 1995 January 1 to 2007 December 31) using Wind measurements. The histogram of the relevant q-metastability measure values is plotted in Figure 4(e). Note that in the H-E (suprathermal) region, the kappa distribution, Equation (2), tends to a power law with the κ-index coinciding with the spectral index in the three-dimensional case, $\kappa = \gamma$ (Livadiotis & McComas 2009, Section 6).

The important results of Dialynas et al. (2009) and Dayeh et al. (2009) drive us to separate the stationary states to those near equilibrium, with $\kappa < \kappa_{Esc}$ (near-equilibrium region), and to those near the q-frozen state, with $\kappa_{Esc} \geqslant \kappa$ (far-equilibrium region or near-q-frozen-state region), where the boundary appears to be somewhere around $\kappa_{Esc} \cong 2.45$. It is interesting that interplanetary (IP) shocks (Desai et al. 2004) and corotating interaction regions (CIRs) (Mason et al. 2008) were found to be characterized by spectral indices in the far-equilibrium region, similar to the results of Dayeh et al. (2009). As we shall see in the following sections, the specific stationary state with the κ-index $\kappa_{Esc} \cong 2.45$, called the escape state, has a key role in the transitions of stationary states. Stationary states can escape from the far-equilibrium region toward the near-equilibrium region, passing through the escape state. This peculiar state has been observed in space plasmas. For example, the energy spectrum of cosmic-ray Fe nucleus has been studied by Sato et al. (1985), where they found the spectral index of Fe being equal to $\gamma \cong -2.45 \pm 0.04$. Also, the most probable value of the κ-index in the Uranian magnetosphere was found to be around the escape value $\kappa_{Esc} \cong 2.45$ that appears from ~7 R_{Io} to ~8 R_{Io} (Mauk et al. 1987). Finally, we point out that the escape value is consistent with the H-E power law of the energetic neutral atoms (ENAs) flux that was recently observed by IBEX toward the heliospheric tail (McComas et al. 2009).

All the above critical values were also found in other plasmas, or plasma-related, slowly driven systems, that emit energy bursts. The emitted photon fluxes obey a power-law energy distribution, which can be explicitly derived from the asymptotic behavior of kappa distributions in the H-E regions. Note also that if $j(\varepsilon)$ is the emitted photon flux, then the emitted energy flux is $\Phi(\varepsilon) = \int j(\varepsilon)\varepsilon d\varepsilon$ (e.g., see Shimizu 1995; Aschwanden et al. 2000).

As an example, solar flares are known to have a power-law energy distribution with reported spectral indices ranging from 1.5 to 2.6 (e.g., see Aschwanden et al. 2000; Charbonneau et al. 2001; Norman et al. 2001). However, if a consistent set of geometrical assumptions is made, the upper value may be reduced from 2.6 to approximately 2.1 (Parnell & Jupp 2000; McIntosh & Charbonneau 2001; McIntosh et al. 2002). On the other hand, the energy distributions of nanoflares are believed to have a different power-law index, namely, larger than 2, though with a large uncertainty (e.g., Benz 2004; Pauluhn & Solanki 2007; Bazarghan et al. 2008), and the same holds for flares that are not associated with CMEs (Yashiro et al. 2006). It can be conjectured that "proper" flares dominate the far-equilibrium region, $\kappa_{Esc} \geqslant \kappa > \frac{3}{2}$, while nanoflares are mostly enclosed in the near-equilibrium region, $\infty \geqslant \kappa > \kappa_{Esc}$. In addition, the statistical analysis of Crosby et al. (1993) of hard X-ray flares detected the spectral index $\gamma \cong 1.62$ for the flares recorded during 1980–1982. This value coincides with $\kappa_{Fund} \cong 1.63$, while for the following years during the decade values closer to the q-frozen state were detected. Kashyap et al. (2002) found that stellar flares are distributed with a power law of the spectral index $\gamma \cong 2.5 \pm 0.4$, that is around the escape value $\kappa_{Esc} \cong 2.45$. Shimizu (1995) studied the active region transient brightenings at the soft X-rays and found a power law with the spectral index ~1.5–1.6. These values are near the q-frozen

state, covering the D-branch of the far-equilibrium region, i.e., between the q-frozen state and the fundamental state.

Close to the fundamental state is also the spectral index $\gamma \cong 1.66$, characterizing the soft gamma repeater bursts (Göğüş et al. 1999). However, spectral indices close to the fundamental state have been observed also in the very H-E gamma-ray sources (Kifune et al. 1995), e.g., in blazar's spectrum, ranging from very low radio frequency to extremely energetic gamma rays. On the other hand, the specific blazar studied in Schroedter et al. (2005) was found to be characterized by the spectral index $\gamma \cong 2.54 \pm 0.18$, which is very close to the escape value $\kappa_{\rm Esc} \cong 2.45$. In general, blazar γ-ray spectral indices were found to be distributed between 1.5 and 2.6 (Von Montigny et al. 1995; Venters & Pavlidou 2007), which coincides with the far-equilibrium region, $\kappa_{\rm Esc} \geqslant \kappa > \frac{3}{2}$. However, the majority of them are distributed near the escape value (Aharonian et al. 2006), e.g., the spectral indices that characterize Markarian 501, which is a bright optical blazar in the core of a giant elliptical galaxy (e.g., see Krennrich et al. 1999).

The q-frozen state was also detected in the X-ray spectra of the accretion disks around Galactic and extragalactic black holes (e.g., Syunyaev et al. 1994). In addition, Ilovaisky et al. (1986) and Miyamoto et al. (1991) found the indices $\gamma \cong 2.27 \pm 0.27$ and $\gamma \cong 2.45 \pm 0.15$, respectively, which are around the escape state of $\kappa_{\rm Esc} \cong 2.45$. It is interesting that when the accretion rate of the disk is very high, the spectral index asymptotically becomes 1.5 (Chakrabarti & Titarchuk 1995) (we recall that the q-frozen state cannot be reached but asymptotically approached). Much earlier, Schreier et al. (1971) detected the q-frozen state in the spectrum of the pulsating X-ray source Cygnus X-1. In particular, the spectral index $\gamma \cong 1.5$ found to characterize the spectra for energies above about 8–9 keV, while for lower energies significant larger values of spectral index were observed, that is $\gamma \geqslant 2.5$, lying thus, on the near-equilibrium region, $\infty \geqslant \kappa > \kappa_{\rm Esc}$. This is not strange, since in the case where the particles are separated into two parts with a different index each (Wang et al. 2003), e.g., $\gamma_1 = 1.5$ and $\gamma_2 = 2.5$, then at low energy values, the steeper spectrum of index $\gamma_2 = 2.5$ controls, while at sufficiently high energy values, the flatter spectrum of $\gamma_1 = 1.5$ index dominates. Finally, we add that the fundamental state was also detected in soft X-rays spectra of Seyfert galaxies, e.g., by Arnaud et al. (1985), where they analyzed observations of the Seyfert 1 galaxy MKN 841.

In Figure 4(f), we illustrate the whole interval of the permissible values of the κ-index, $\kappa \in (\frac{3}{2}, \infty]$, (or, of the q-indices, $q \in [1, \frac{5}{3})$), that is $M_q \in [0\%, 100\%)$ in terms of the deviation measure values. The specific values discussed in this section of $\kappa_{\rm EQ} = \infty$, $\kappa_{\rm Esc} \cong 2.45$, $\kappa_{\rm Fund} \cong 1.63$, and $\kappa_{\rm q-F} \cong 1.5$, are also indicated.

5. THE ENTROPY OF A STATIONARY STATE

5.1. Derivation and Survey

Having identified the entire set of stationary states that cover the interval $\kappa \in (\frac{3}{2}, \infty]$, we are now interested in finding the entropy that would characterize the system in each of these stationary states. As we have already discussed, the temperature is a parameter that does not affect the value of the κ-index. Namely, by simply varying the temperature, while retaining a fixed value of q-index (that is fixed κ-index, and q-metastability measure since the dimensionality of the system is constant), the system should remain in the same stationary state (iso-metastability procedure). On the other hand, by varying the κ-index (or equivalently, the q-index or the M_q measure), the system can transit through various stationary states without any variation of the temperature (isothermal procedure). Thus, the entropy we wish to find should be dependent only on the value of the κ-index (or, q-index, M_q), and independent of the temperature.

The Tsallis entropy for the continuous description of data is written as

$$S_q[p] \equiv \frac{1 - \phi_q[p]}{q - 1}, \tag{19}$$

with the argument ϕ_q given by

$$\phi_q[p] \equiv \int_{V_u} \left[p(\vec{w}) \cdot \sigma^f\right]^q \frac{dw_1 dw_2 \ldots dw_f}{\sigma^f}, \tag{20}$$

where $\vec{w} \equiv \vec{u} - \vec{u}_b$ spans the velocity subspace $\mathcal{V}_u \subseteq \Re^f$ and σ is a characteristic speed-scale of the system as defined and used by Tsallis and co-workers (Tsallis et al. 1995; Prato & Tsallis 1999; Tsallis 1999; 2009); it is important to note that in this study σ is used solely for this speed-scale and has nothing to do with the standard deviation, which uses the same symbol. $p(\vec{w})$ is called the ordinary probability distribution and is related to the escort distribution as $P(\vec{w}) \sim p(\vec{w})^q$. Given the spherical symmetry $p(\vec{w}; \theta_{\rm eff}; q) = p(w; \theta_{\rm eff}; q)$, the argument ϕ_q is

$$\phi_q \equiv \int_0^\infty [p(w; \theta_{\rm eff}; q) \cdot \sigma^f]^q \cdot \frac{g_{\rm V}(w) dw}{\sigma^f}. \tag{21}$$

For $f = 3$, Livadiotis & McComas (2009) showed that

$$p(\vec{w}; \theta_{\rm eff}; q) = \theta_{\rm eff}^{-3} \cdot \frac{1}{2\pi} \cdot \frac{1}{1_q\left(\frac{3}{2}\right)^{\frac{3}{2}} \tilde{\Gamma}_q\left(\frac{3}{2}\right)} \cdot \exp_q\left[-\frac{1}{1_q\left(\frac{3}{2}\right)} \cdot \left(\frac{\vec{w}}{\theta_{\rm eff}}\right)^2\right], \tag{22}$$

and that the extracted argument ϕ_q is given by

$$\phi_q(q; T_q; \sigma) = 1_q\left(\frac{3}{2}\right)^{1_q\left(\frac{1}{2}\right)} \cdot \left[2\pi \Gamma_q\left(\frac{3}{2}\right)\right]^{1-q} \cdot \left(\frac{2k_B}{\sigma^2 \mu} T_q\right)^{\frac{3}{2}(1-q)}. \tag{23}$$

The functions $\tilde{\Gamma}_q(a)$ and $\Gamma_q(a)$ are the q-deformed Gamma functions of the first and second kinds. These were defined and studied in Livadiotis & McComas (2009, Appendix A), namely,

$$\tilde{\Gamma}_q(a) \equiv \int_0^\infty \exp_q(-y) y^{a-1} dy = \int_0^\infty [1 - (1-q)y]_+^{\frac{1}{1-q}} y^{a-1} dy, \tag{24}$$

$$\Gamma_q(a) \equiv \int_0^\infty \exp_q(-y) y^{a-1} dy = \int_0^\infty [1 - (1-q)y]_+^{\frac{q}{1-q}} y^{a-1} dy, \tag{25}$$

where $\exp_q(x) \equiv [1 + (1-q)x]_+^{\frac{1}{1-q}}$ denotes the q-deformed exponential function (e.g., Silva et al. 1998; Yamano 2002), while the subscript "+" denotes the operation $[x]_+ = x$, if $x \geqslant 0$ and $[x]_+ = 0$, if $x \leqslant 0$, in accordance with the Tsallis cut-off

condition. Both kinds of q-deformed Gamma functions recover the ordinary gamma function $\Gamma(a)$ for $q \to 1$. Notation of the q-deformed "unit function," $1_q(u) \equiv 1+(1-q)u$, which is also introduced in (Livadiotis & McComas 2009). For $a = \frac{3}{2}$, we obtain

$$\Gamma_q\left(\frac{3}{2}\right) = \tilde{\Gamma}_q\left(\frac{3}{2}\right) \cdot 1_q\left(\frac{3}{2}\right) = \frac{\sqrt{\pi}}{2} \cdot (q-1)^{-\frac{1}{2}} \cdot \frac{\Gamma\left(\frac{1}{q-1} - \frac{1}{2}\right)}{\Gamma\left(\frac{1}{q-1}\right)}. \quad (26)$$

Now we address the issue of the physical meaning of the speed-scale parameter σ. Equation (23) clarifies that the argument ϕ_q depends on the q-index and the dimensionless quantity $2k_B/(\sigma^2\mu) \cdot T_q$. According to Tsallis (Tsallis et al. 1995; Prato & Tsallis 1999; Tsallis 1999, 2009), the σ parameter depends on the characteristics of the given problem. Here, instead of relating σ to quantities having velocity dimensions, we equivalently relate $\sigma^2\mu/(2k_B)$ to quantities having temperature dimensions. Further, given the three definitions of temperature (see the introduction), we can potentially have three different interpretations of $\sigma^2\mu/(2k_B)$. Namely, we deal with the following temperature/temperature-like parameters: (1) the thermodynamic (physical temperature) T_q, (2) the kinetic, T_K, and (3) the Lagrangian, T.

In the classical case when systems are assumed to be at equilibrium, all the three definitions are equivalent, i.e., $T_q = T_K = T$, and thus, only one, trivial interpretation appears: $\sigma^2\mu/(2k_B) = T_q = T_K = T$. Namely, the dimensionless quantity is simply $2k_B/(\sigma^2\mu) \cdot T_q = 1$. However, for stationary states out of equilibrium, the equality holds only between the first two definitions, $T_q = T_K$. Hence, now we have two possible interpretations. Namely, (1) $\sigma^2\mu/(2k_B) = T_q$. This is the same as the classical case at equilibrium. Namely, the dimensionless quantity is $2k_B/(\sigma^2\mu) \cdot T_q = 1$. (2) $\sigma^2\mu/(2k_B) = T$. This is a novel interpretation, since T is dependent parameter, namely, $T = T(T_q; q)$. The connecting function can be found easily through a relation that is well known in non-extensive statistical mechanics, i.e., $T = T_q/\phi_q$; namely, the dimensionless quantity is $2k_B/(\sigma^2\mu) \cdot T_q = \phi_q$. Hence, we have two possible interpretations:

$$(1) \quad \sigma^2\mu/(2k_B) = T_q, \text{ or, } 2k_B/(\sigma^2\mu) \cdot T_q = 1 \quad \text{and} \quad (27)$$

$$(2) \quad \sigma^2\mu/(2k_B) = T, \text{ or, } 2k_B/(\sigma^2\mu) \cdot T_q = \phi_q. \quad (28)$$

Let us start by discussing the first interpretation (Equation (27)); by setting $\sigma^2\mu/(2k_B) = T_q$ in Equation (23), we have

$$\phi_q(q) = 1_q\left(\tfrac{3}{2}\right)^{1_q\left(\frac{1}{2}\right)} \cdot \left[2\pi\Gamma_q\left(\tfrac{3}{2}\right)\right]^{1-q}. \quad (29)$$

In this way, the argument ϕ_q depends only on the q-index that characterizes a particular stationary state, and thus, the same holds for the entropy S_q, i.e.,

$$S_q(q) = \frac{1 - 1_q\left(\tfrac{3}{2}\right)^{1_q\left(\frac{1}{2}\right)} \cdot \left[2\pi\Gamma_q\left(\tfrac{3}{2}\right)\right]^{1-q}}{q-1}. \quad (30)$$

Note that for the specific stationary state at equilibrium ($q = 1$), the entropy is trivially given by the BG entropy, that is

$$S_{EQ} \equiv S_q(q=1) = \frac{3}{2} \cdot [1 + \ln(\pi)] \cong 3.2171. \quad (31)$$

On the other hand, for the q-frozen stationary state ($q \to \frac{5}{3}$), the argument ϕ_q equals zero, and trivially the entropy of this extreme state becomes

$$S_{q-F} \equiv S_q\left(q \to \frac{5}{3}\right) = \frac{3}{2}. \quad (32)$$

In the whole interval $q \in [1, \frac{5}{3})$, and as q decreases, the entropy increases monotonically from its minimum value S_{q-F} to its maximum S_{EQ}.

In the second interpretation (Equation (28)), we use the only temperature-like quantity emerging from statistics, the inverse of the second Lagrangian multiplier, that is to say $\sigma^2\mu/(2k_B) = T$. Then, given Equation (23) and that T is expressed in terms of the physical temperature T_q as $T = T_q/\phi_q$, we conclude that

$$\phi_q(q) = \left\{1_q\left(\frac{3}{2}\right)^{1_q\left(\frac{1}{2}\right)} \cdot \left[2\pi\Gamma_q\left(\frac{3}{2}\right)\right]^{1-q}\right\}^{\frac{1}{1_q(-\frac{3}{2})}} \quad (33)$$

and

$$S_q(q) = \frac{1 - \left\{1_q\left(\tfrac{3}{2}\right)^{1_q\left(\frac{1}{2}\right)} \cdot \left[2\pi\Gamma_q\left(\tfrac{3}{2}\right)\right]^{1-q}\right\}^{\frac{1}{1_q(-\frac{3}{2})}}}{q-1}. \quad (34)$$

Now the entropy is not increasing monotonically over the whole interval $q \in [1, \frac{5}{3})$. In particular, as the q-index decreases starting from the q-frozen state to equilibrium, the entropy decreases from $S_{q-F} = 1.5$ until a minimum at $q_{Fund} \cong 1.6125$ (corresponding to $\kappa_{Fund} \cong 1.6327$ and $M_{q,Fund} = 93.780\%$) with entropy $S_{Fund} \cong 1.2856$. The minimum value of entropy defines a "fundamental" stationary state. The new interesting features that characterize only the second interpretation of entropy (e.g., the non-monotonicity, the cavity, a deceleration branch in addition to the acceleration one) appear because the fundamental state does not coincide with the extreme, q-frozen state, as it is in the first interpretation.

After the entropic minimum and as the q-index continues to decrease, the entropy starts to increase until it reaches equilibrium at $S_{EQ} \cong 3.2171$. Both the entropic behaviors of Equations (30) and (34) are plotted in Figure 5. In this figure, the first interpretation (Equation (27)), $\sigma^2\mu/(2k_B) = T_q$, which leads to the entropy expression of Equation (30), is represented by the blue dash line, while the non-monotonic entropy expression of Equation (34), which follows from the second interpretation (Equation (28)), $\sigma^2\mu/(2k_B) = T$, is represented by the red solid line.

Under spontaneous procedures that increase the system's entropy, the first interpretation (Equation (27)) leads to a monotonically decreasing q-index. On the other hand, the second interpretation (Equation (28)) suggests a significantly different and more interesting behavior. Indeed, starting from the fundamental state, i.e., with minimum entropy S_{Fund}, the spontaneous entropic augments can now produce either a monotonically decreasing q-index along the left-hand side branch of $q < q_{Fund}$, or a monotonically increasing q-index along the right-hand side branch of $q > q_{Fund}$. Ultimately, the decreasing q-index will reach its equilibrium value at $q = 1$, and the increasing q-index will approach the q-frozen state at $q \to \frac{5}{3}$. While the former behavior can be decreasing without any barrier in the interval from $q = q_{Fund}$ to $q = 1$, the latter behavior

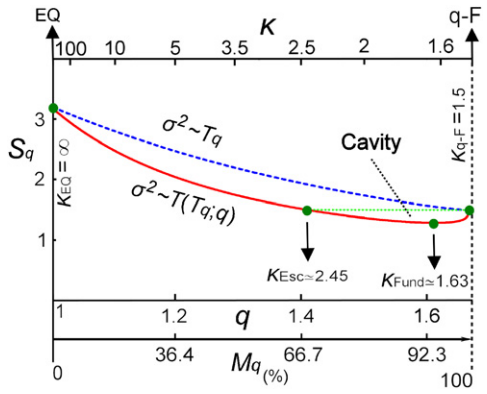

Figure 5. Tsallis entropy, S_q, calculated for the Tsallis–Maxwellian distribution of velocities, and depicted with respect to the q- and κ-indices, and the q-metastability measure M_q. The entropy is shown for both the interpretations (Equation (27)) and (Equation (28)). The cavity that is the non-monotonic part of the entropy, $\kappa_{\rm Esc} \geqslant \kappa > \frac{3}{2}$ in the second interpretation, can explain the observed κ-index values of $\kappa_{\rm Esc} \cong 2.45$ and $\kappa_{\rm Fund} \cong 1.63$, and their dynamic relation with the extreme values of $\kappa_{\rm EQ} = \infty$ and $\kappa_{\rm q-F} \cong 1.5$.

takes place as far as the increasing q-index approaches the q-frozen state at $q \to \frac{5}{3}$. Then, any further augments of entropy can occur only due to isentropic procedures (as we describe in the following section) that allow transitions between the two branches. Such procedures will divert the q-index from $q \to \frac{5}{3}$ to $q = q_{\rm Esc} \cong 1.4082$, where it can keep decreasing along the left-hand branch. The critical point at $q_{\rm Esc} \cong 1.4082$ (corresponding to $\kappa_{\rm Esc} \cong 2.450$ and $M_{q,{\rm Esc}} \cong 67.80\%$) separates the interval $q \in [1, \frac{5}{3})$ into two parts, namely, $q \in [1, q_{\rm Esc})$, in which the entropy S_q is a bijective function of q-index, and $q \in [q_{\rm Esc}, \frac{5}{3})$, in which the entropy S_q is only a surjective function since the one-to-one correspondence is lost. As we shall see in the following section, the cavity that is enclosed in the subinterval $q \in [q_{\rm Esc}, \frac{5}{3})$ can host isentropic procedures.

It is remarkable that under the second interpretation (Equation (28)) both the predicted critical values of $\kappa_{\rm Esc} \cong 2.450$ and $\kappa_{\rm Fund} \cong 1.6327$ are observed in space plasmas. The former constitutes a separator between the stationary states near equilibrium and those near the q-frozen state (e.g., see the analyses of Dialynas et al. 2009; Dayeh et al. 2009; see also Section 4.3). The latter value minimizes the entropy and coincides with the value estimated by the work of Decker et al. (2005). External factors that can decrease the entropy of the system move it into a different stationary state, closer to the fundamental state. In the case of solar wind, for example, newly formed pick-up ions may play just such a role because their motion is highly ordered. This motion is dictated by the relative orientation of the solar wind velocity vector and the interplanetary magnetic field, which become increasingly perpendicular on average as one moves out through the heliosphere.

After ionization, the pick-up ions gyrate about the solar wind magnetic field, with their guiding center moving at the solar wind velocity, forming a ring velocity distribution. Very quickly, these ions are scattered by self-generated Alfvenic fluctuations, forming spherical shell distributions, centered approximately at the solar wind velocity with a radius of the solar wind speed (e.g., Sagdeev et al. 1986; Lee & Ip 1987). The hybrid probability distribution, which is a normalized sum of both the kappa distribution of the original stationary state and the spherical shell distribution, describes a more organized state. Therefore, this hybrid state should have less entropy than the stationary state assigned by the original kappa distribution. As the pick-up ions co-move with the solar wind, they undergo adiabatic cooling, which reduces the radius of the shell (Zilbersher & Gedalin 1997). In this way, pick-up ions move from the shell distribution and merge with the original particles into a new kappa distribution. Thus, the hybrid state transits to a new stationary state with a different kappa and lower entropy. The departure of the pick-up ions from the spherical distribution to the solar wind new stationary state can re-increase the entropy. However, this procedure is much slower, so that the whole transition of the original to the new stationary state can be characterized by a decrease of entropy. In this model, the hybrid state is transient, tending finally to a new stationary state with lower entropy than the original stationary state, closer to the fundamental state.

Following this reasoning, in the distant solar wind of the outer heliosphere, where pick-up protons represent an increasing fraction of the population, the entropy can become smaller and the specific stationary state with the lowest entropy becomes achievable. If the first interpretation (Equation (27)) is applied, then the effect of pick-up ions leads to the q-frozen state and internal increases of entropy would direct the system again back to equilibrium. On the other hand, if the second interpretation (Equation (28)) is applied, then the effect of pick-up ions leads to the fundamental state. In this case, the internal increases of entropy would direct the system both toward the q-frozen state and equilibrium (Section 6).

While the first interpretation of Equation (27) was used to describe diffusion processes within the framework of Tsallis statistical mechanics (e.g., Tsallis et al. 1995; Prato & Tsallis 1999), there are a number of good reasons to believe that the second interpretation of Equation (28) is also physically meaningful and may have important implications in at least some physical systems including space plasmas:

1. The critical value of the κ-index $\kappa_{\rm q-F} \cong 1.5$, which is a limiting value in both interpretations, should be difficult to observe in the first interpretation (Equation (27)) as any increase in entropy drives systems away from this particular stationary state. In contrast, Fisk & Gloeckler (2006) claim this to be almost "ubiquitously" observed in space plasmas, suggested that systems might collect at this value, rather than moving away from it. Interpretation (Equation (28)) provides a natural explanation for just this sort of collection at $\kappa_{\rm q-F} \cong 1.5$ as increases in entropy lead to this value along the D-branch.
2. The critical values of the κ-index that arise from interpretation (Equation (28)) have been routinely observed in space plasmas: $\kappa_{\rm Fund} \cong 1.63$ and $\kappa_{\rm Esc} \cong 2.45$, in addition to $\kappa_{\rm EQ} = \infty$ and $\kappa_{\rm q-F} \cong 1.5$ (that arise from interpretation (Equation (27)). These critical values of the κ-index are also related to certain dynamical behavior. Starting from (or near) the fundamental state, $\kappa_{\rm Fund} \cong 1.63$, the system transits to various stationary states before finally reaching equilibrium $\kappa_{\rm EQ} = \infty$ (Section 6).
3. Significantly different dynamical behavior characterizes the near- and far-equilibrium stationary states. The separator $\kappa_{\rm Esc} \cong 2.45$ is the escape point of stationary states from the non-monotonic entropic cavity of $\kappa_{\rm Esc} \geqslant \kappa > \frac{3}{2}$ to the monotonic entropic behavior of $\infty \geqslant \kappa > \kappa_{\rm Esc}$. Inside the cavity, the system can approach this escape point either directly, through a specific stochastic acceleration process, or indirectly, interceding the q-frozen state, $\kappa_{\rm q-F} \cong 1.5$, through an opposite stochastic deceleration. This exposed

dynamical scenario is also supported by observations. While the extreme states of equilibrium, $\kappa_{EQ} = \infty$, and of the q-frozen state, $\kappa_{q-F} \cong 1.5$, are both observed in the inner heliosphere, the fundamental state, $\kappa_{Fund} \cong 1.63$, was detected in the distant solar wind of the outer heliosphere, where the influence of pick-up ions in minimizing entropy, for example, should be stronger (see Table 1). In the presence of internal irreversible procedures that increase entropy, and in the absence of any external procedure that decreases entropy, plasmas are expected to be characterized by stationary states that lie in the near-equilibrium region, $\infty \geqslant \kappa > \kappa_{Esc}$. However, when the internal procedures that increase entropy are rare, e.g., in the quiet times of the solar wind (e.g., Dayeh et al. 2009), plasmas can be characterized by stationary states that lie in the far-equilibrium (or, near-q-frozen-state) region, $\kappa_{Esc} \geqslant \kappa > \frac{3}{2}$.

4. The above critical values were also found in other plasmas, or plasma-related, slowly driven systems, that emit energy bursts as is shown in Section 4.3 and Table 1.
5. The connection of the only temperature-like quantity emerging from statistics, the inverse of the second Lagrangian multiplier, to the speed-scale σ (28), is mathematically permissible as the second Lagrangian multiplier specifically characterizes the distribution of velocities in a system. In physics, it is rare to find mathematically permissible behaviors that are observable but ultimately never observed.

In the following, we describe the entropy configuration in the whole interval of stationary states $q \in [1, \frac{5}{3})$, according to the second interpretation, and the dynamical behavior that follows from this specific configuration. In Section 6, we deal with the dynamics of the transition of stationary states and show the detailed paths by which the transition of stationary states evolves toward equilibrium.

5.2. Spontaneous Entropic Procedures

Having expressed the entropy of stationary states as a function of the q-index, we are ready to examine how the spontaneous entropic variations will affect the values of this index. Any internal procedure is supposed to either increase (irreversible procedures), or preserve (reversible procedures) the entropy of the system. As soon as the system is in stationary states outside the cavity, i.e., $q \in [1, q_{Esc})$, a specific value of entropy corresponds to a specific value of the q-index (one-to-one relation). Augments of entropy lead the system to transit through stationary states of a smaller q-index toward equilibrium. On the other hand, when the system is in stationary states that are located inside the cavity, i.e., $q \in [q_{Esc}, \frac{5}{3})$, a specific value of entropy corresponds to two values of the q-index. Then, isentropic transitions might also take place.

As we observed in Figure 5, the depicted entropy $S_q(q)$ is a non-monotonic function inside the cavity, that is for values of entropy $S_{Fund} \leqslant S \leqslant 1.5$ and the q-index $q_{Esc} \leqslant q < \frac{5}{3}$. Thus, the entropy is characterized by two monotonic branches: the acceleration A-branch for $q_{Esc} \leqslant q \leqslant q_{Fund}$ with entropy $S_{q,A}(q)$ and the deceleration D-branch for $q_{Fund} \leqslant q < \frac{5}{3}$ with entropy $S_{q,D}(q)$. Note that the A-branch extends out of the cavity all the way to equilibrium ($q = 1$). As q increases, the entropy on the A-branch, $S_{q,A}(q)$, decreases, approaching the minimum value $S_{q,A}(q) = S_{Fund}$ with index $q = q_{Fund}$, while on the D-branch, the entropy $S_{q,D}(q)$ increases, deviating from the minimum value S_{Fund} and the index q_{Fund}, and approaching $S_{q,D}(q) \to 1.5$, or $q \to \frac{5}{3}$. In other words, as soon as the entropy increases, the A-branch $S_{q,A}(q)$ is leading to a decrease of q (decrease of M_q, increase of κ), while the D-branch $S_{q,D}(q)$ is leading to an increase of q (increase of M_q, decrease of κ). Therefore, along the A-branch, spontaneous entropic increments lead to smaller q-indices and the stationary states transit gradually to equilibrium ($q = 1, \kappa = \infty, M_q = 0\%$). This procedure is related to an isothermal shifting of the energy probability distribution to higher energy values, as shown in Figures 2(a) and (c) (stochastic acceleration). On the other hand, along the D-branch, spontaneous entropic increments lead to larger q-indices, and thus, the relevant transition of stationary states lead gradually to the largest deviation from equilibrium, the q-frozen state ($q \to \frac{5}{3}, \kappa \to \frac{3}{2}, M_q \to 100\%$). This procedure is related to an opposite isothermal shifting of the energy probability distribution toward lower energy values (stochastic deceleration).

The cavity enclosed by both the A- and D-branches for $S_{Fund} \leqslant S \leqslant 1.5$ is of great interest. Even though, the system can transit to stationary states of higher entropy, a specific isentropic transition should also be possible. This can be realized by the two solutions of the equation $S_q(q) = \text{constant} \equiv S \leqslant 1.5$, namely, $q_A = S^{-1}_{q,A}(S)$ (along the A-branch) and $q_D = S^{-1}_{q,D}(S)$ (along the D-branch). Then, the isentropic switching of the system between the two stationary states of deviation measures q_A and q_D is possible, as soon as the entropy is $S_{Fund} \leqslant S_q \leqslant 1.5$, namely, it is included within the cavity (or equivalently, the q-metastability measure is $M_{q,Esc} \leqslant M_q < 100\%$, or the q-, κ-indices are $q_{Esc} \leqslant q < \frac{5}{3}, \kappa_{Esc} \geqslant \kappa > \frac{3}{2}$). The isentropic switching of the system can be represented by the dual function $d_q(q)$, where, by duality we mean the property $d^2(x) = d\,(d(x)) = x$, for $x \in \Re$. Namely,

$$q_D = d_q(q_A),\ q_A = d_q(q_D),\ \text{with } d_q(q) = \begin{cases} (S^{-1}_{q,A} \circ S_q)(q) & \text{if } q \geqslant q_{Fund}\ (D-\text{branch}), \\ (S^{-1}_{q,D} \circ S_q)(q) & \text{if } q \leqslant q_{Fund}\ (A-\text{branch}). \end{cases} \quad (35)$$

We stress the fact that the isentropic switching is not a procedure that takes place instantly, which would require a huge instantaneous transfer of energy from (or to) the "far tail" particles with the κ-index close to the q-frozen state to (or from) the bulk of the distribution at lower energies. This incorrect impression might appear, since the exact meaning of Equation (35) is to describe transitions only between stationary states, and ignores all the intermediate non-stationary states that occur between them. In this way, the deformation of distributions during the isentropic switching is a finite time process whose end points are described by Equation (35) as the initial and final stationary states of this switching. It is not the purpose of this paper to give detailed descriptions of the physical processes that accomplish isentropic switching, or to address the timescales of this or other transitions between the stationary states.

The transition of the system through various stationary states along the A- and D-branches results in the extreme stationary states at equilibrium and the q-frozen state, respectively. However, the isentropic switching allows all stationary states to eventually reach equilibrium, because all the stationary states that are accumulated near the q-frozen state are eventually diverted to the escape state ($q_{Esc} \cong 1.4082$, $\kappa_{Esc} \cong 2.450$, $M_{q,Esc} \cong 67.80\%$), namely, to the separator of the stationary states near equilibrium and those near q-frozen state. As the entropy keeps increasing

out of the cavity, the transition takes place along the A-branch. Therefore, the A-branch for $M_q < M_{q,\mathrm{Esc}}$ (outside the cavity) is the ultimate fate followed by all stated regardless of whether they followed by the A- or D-branch inside the cavity. This dynamical behavior of the transient stationary states is the subject of Section 6.

6. THE DISCRETE DYNAMICS OF TRANSITIONS BETWEEN STATIONARY STATES

6.1. Discrete Dynamics

The description of stationary states out of equilibrium within the framework of Tsallis statistical mechanics is a static theory. The stationary probability distribution, which is the kappa distribution, is extracted by extremizing the Tsallis entropy under the constraints of canonical ensemble. However, this procedure in no way examines the dynamical behavior of the system's arrival at (or departure from) these Tsallis-like stationary states that fill the interval $\kappa \in (\frac{3}{2}, \infty]$ (or, $q \in [1, \frac{5}{3})$, $M_q \in [0\%, 100\%)$). In the case where the stationary state is the specific one at equilibrium, the dynamical behavior of systems approaching (or leaving) equilibrium is given by the well-known Vlasov–Maxwell differential equations (specified by Parker's equation for the solar wind). The extracted solution describes the time-dependent probability distribution of particles in the phase space, $p(\vec{x}; \vec{w}; t)$, under the initial condition of a Maxwellian $p(\vec{x}; \vec{w}; t = 0) = P(\vec{w}; \theta_{\mathrm{eff}}; \kappa = \infty)$. Obviously, the solution $p(\vec{x}; \vec{w}; t)$ refers either to the system's departure from equilibrium, for $t > 0$, or to its arrival to equilibrium, for $t < 0$. In a similar way, one can study the dynamical behavior of the system's approaching (or leaving) stationary states out of equilibrium. In this case, the initial probability distribution is given by a kappa distribution, namely, $p(\vec{x}; \vec{w}; t = 0) = P(\vec{w}; \theta_{\mathrm{eff}}; \kappa)$ for any permissible value of the κ-index in the interval $\kappa \in (\frac{3}{2}, \infty]$. Interestingly, Prested et al. (2008), Heerikhuisen et al. (2008), and Schwadron et al. (2009) used as initial probability distribution the specific kappa distribution with $\kappa = \kappa_{\mathrm{Fund}} \cong 1.63$; this coincides with our approach, where the starting point of the transient stationary states is the fundamental state, namely for that κ-index for which the entropy is minimized.

In our approach, we consider that the system transits through a number N_{ss} of alternating stationary states. Each stationary state is assigned by a kappa distribution of a specific κ-index (q-index, or measure M_q). Hence, the evolution of the system, during its transition into these N_{ss} stationary states, is interpreted by the set of kappa distributions $\{P(\vec{w}; \theta_{\mathrm{eff}}; \kappa_n)\}_{n=0}^{N_{\mathrm{ss}}}$, in which the index n counts the various states, with $n = 0$ and $n = N_{\mathrm{ss}}$, corresponding to the initial and final stationary states, respectively. In this way, the continuous time that is included in Vlasov's, Parker's, or other stochastic equations, $p(\vec{x}; \vec{w}; t)$, is now replaced by the index $n = 0, 1, 2, \ldots, N_{\mathrm{ss}}$, that has the role of the discrete time.

Precisely speaking, a differential equation with respect to time t, as well as its solution in the time interval $t \in [0, t_f]$, can always be "discretized" by considering a finite step of time δt, so that, $t = n \cdot \delta t$, with $n = 0 \Leftrightarrow t = 0$, $n = N_{ss} \Leftrightarrow t = t_f = N_{ss} \cdot \delta t$. Then, the differential equation degenerates to what is called "difference equation" (e.g., Elaydi 2005), that is a recurrent relation (a map, multi-dimensional in the generic case) of the $(n+1)$th arguments and parameters of the distribution (e.g., the κ-index) to the nth respective ones ($\kappa_{n+1} = \kappa_{n+1}(\kappa_n)$). Specifically, the discrete approach neglects the times of the sequential departures (and arrivals) of the system at each one of the N_{ss} metastable stationary states, while focusing instead on the sequential stationary states themselves. Most important is the fact that at each discrete time, $n = 0, 1, 2, \ldots, N_{\mathrm{ss}}$, the attained stationary state is a kappa distribution, where the κ-index is the only changing parameter, so that all information about the dynamics is included in the discrete time dependence of kappa indices $\{\kappa_n\}_{n=0}^{N_{\mathrm{ss}}}$ (or equivalently, $\{q_n\}_{n=0}^{N_{\mathrm{ss}}}$ and $\{M_{q,n}\}_{n=0}^{N_{\mathrm{ss}}}$).

6.2. The Discrete Map of Stationary States Transitions

We demonstrate the transition of stationary states toward equilibrium and the q-frozen state by examining the simplest case where all of the internal procedures that the system is subject to lead to equal augments of entropy δS, that is

$$S_{q,n+1} \equiv S_{q,n} + \delta S, \quad \forall\, n = 0, 1, 2, \ldots, N_{\mathrm{ss}} - 1. \tag{36}$$

Then, the relevant values of the q-index $\{q_n\}_{n=0}^{N_{\mathrm{ss}}}$ are given by

$$q_{n+1} = f_q(q_n), \text{ with } f_q(q) \equiv \begin{cases} S_{q,\mathrm{D}}^{-1}[S_q(q) + \delta S] & \text{if } q \geqslant q_{\mathrm{B}} \ (D\text{−branch}), \\ S_{q,\mathrm{A}}^{-1}[S_q(q) + \delta S] & \text{if } q \leqslant q_{\mathrm{B}} \ (A\text{−branch}), \end{cases} \tag{37}$$

The transition of stationary states toward equilibrium along the A-branch and toward the q-frozen state along the D-branch can be shown in a special diagram called discrete phase space of the map (Equation (37)). This is the plot of all the pairs (q_n, q_{n+1}) of the map $q_n \to q_{n+1} = f_q(q_n)$, $\forall n = 0, 1, 2, \ldots$. The sequence of the q-index values q_0, q_1, q_2, and so on, is formed by the iterations of the map (Equation (37)). Each of the iterations $n = 0, 1, 2, \ldots$ is geometrically represented by a horizontal line segment from the graph of the map $f_q(q)$ to the bisector, followed by a vertical line segment from the bisector back to the map. In Figure 6, we present the phase-space portrait for transient stationary states along the A-branch, i.e., the initial value of q-index is $q_0 < q_{\mathrm{Fund}}$, where we choose $q_0 = 1.6$, and along the D-branch, i.e., the initial value of the q-index is $q_0 > q_{\mathrm{Fund}}$, where we choose $q_0 = 1.62$. (We choose the initial value q_0 to be lying near the value q_{Fund} of the fundamental state.) Along the D-branch and when the values of the q-index become sufficiently close to the q-frozen state, let this be the $(n_{\mathrm{q-F}})$th iteration, i.e., $q_{n_{\mathrm{q-F}}} \cong \frac{5}{3}$, then, in the next, $(n_{\mathrm{q-F}} + 1)$th iteration, an isentropic switching shifts the value of the q-index out and near the edge of the cavity, namely, $q_{n_{\mathrm{q-F}}+1} \cong q_{\mathrm{Esc}}$. Of course, isentropic switching back and forth is possible everywhere within the cavity, but only leads in a unique direction as particles switch from near the q-frozen state to where they can escape out of the cavity. Here we have $n_{\mathrm{q-F}} = 3$, and thus, from the 4th iteration and beyond, the dynamical behavior is similar to that of the case $q_0 < q_{\mathrm{Fund}}$.

6.3. Numerical Application of the Discrete Transitions of Stationary States

In the following, we apply the map (Equation (37)) to demonstrate the transition of stationary states within the framework of the discrete approach (as explained in Section 6.1) and their accumulation to the extreme states of equilibrium and q-frozen state.

In our numerical calculation, the initial values of the map (Equation (37)) are randomly equidistributed in the interval $[q_{\mathrm{Fund}} - \delta q, q_{\mathrm{Fund}} + \delta q]$, with $\delta q \equiv 0.1 \cdot (\frac{5}{3} - q_{\mathrm{Esc}}) \cong 0.0258$.

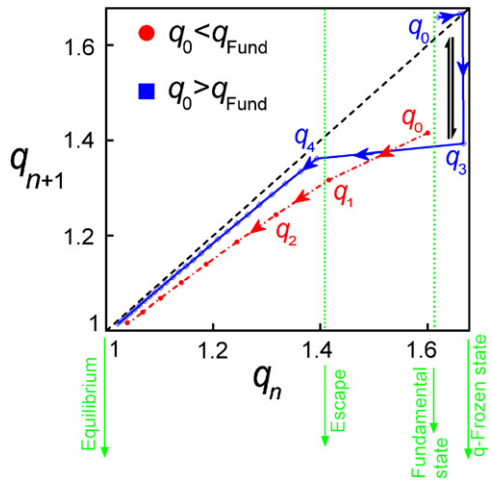

Figure 6. Phase-space portrait for transient stationary states along the A-branch with $q_0 = 1.6 < q_{\rm Fund}$ and (constant) entropic step $\delta S = 0.2$ (red dash-dot line), and along the D-branch with $q_0 = 1.62 > q_{\rm Fund}$ and $\delta S = 0.06$ (blue solid line). In this case, when the values of the q-index become sufficiently close to the q-frozen state, that is in the $n_{\rm q-F}$th iteration ($n_{\rm q-F} = 3$), then, in the next, $(n_{\rm q-F} + 1)$th iteration, the isentropic mechanism shifts the value of the q-index out and near the edge of the cavity, namely, $q_{n_{\rm q-F}+1} \cong q_{\rm Esc}$. The isentropic switching is possible for any state within the cavity (black vertical arrows).

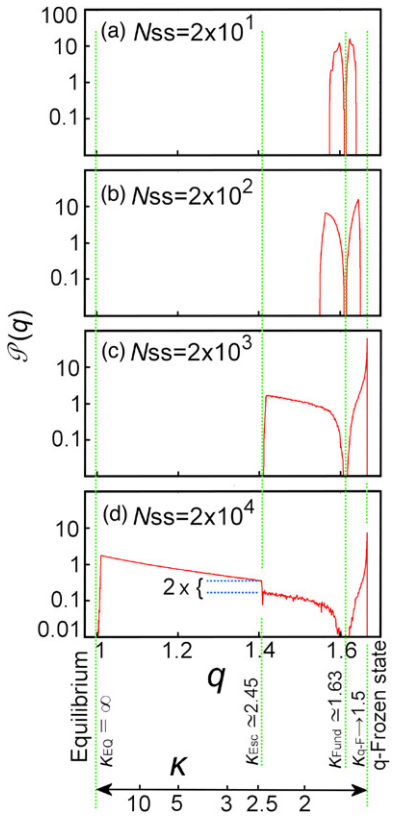

Figure 7. Probability distribution $P(q)$ is depicted for different number of iterations in our numerical simulation, i.e., (a) $N_{\rm ss} = 2 \times 10$ (10^4 initial values), (b) $N_{\rm ss} = 2 \times 10^2$ (10^3 initial values), (c) $N_{\rm ss} = 2 \times 10^3$ (10^2 initial values), and (d) $N_{\rm ss} = 2 \times 10^4$ (10 initial values). The extreme states of equilibrium and q-frozen state, the A- and D-branches, as well as the separator point $q_{\rm Esc}$, are indicated. For small numbers of iterations (a)–(c) where the stationary states are distributed only in the far-equilibrium region, then the q-frozen state acts as an "attractor," i.e., the states are accumulated close to the q-frozen state. However, for a sufficiently large number of iterations, the q-frozen state drains, as states near the q-frozen state undergo isentropic transitions and escape toward equilibrium. The factor of 2 at $\kappa = \kappa_{\rm Esc}$ comes from our assumption of switching, on average, every other time step.

Each initial value is iterated N_{ss} times with the map (Equation (37)) with the entropic step $\delta S = 10^{-4}$. Hence, N_{ss} transient stationary states are reached, and the relevant N_{ss} different values of the q-index are recorded.

We also allow isentropic switching (according to Equation (35)) to take place after each transition of the system between two sequential stationary states. The choice of isentropic switching is randomly returned. Namely, after each transition $q_n \rightarrow q_{n+1} = f_q(q_n)$, the isentropic switching is applied $q_{n+1} \rightarrow d_q(q_{n+1})$, if a binary random variable, called "iso-S", returns iso-$S = 1$, while it is not applied when iso-$S = 0$.

Furthermore, we assume that the system is affected by the exterior factor that minimizes its entropy after the passage of $N_{\rm ss}$ steps. Therefore, the entropy is gradually increasing within $(N_{ss} - 1)$ steps, followed by an abrupt decrease in the $N_{\rm ss}$th step. The rejuvenation of the system's entropy leads to a value that is chosen to be randomly equidistributed close to the entropy minimum value (close to the fundamental state). Each of these rejuvenated entopic values is treated as a different initial value in the map (Equation (37)). This cycle that involves certain $(N_{ss} - 1)$ entropic gradual increments and one abrupt decrement is repeated for $2 \times 10^5 / N_{\rm ss}$ times, that is, a number of $2 \times 10^5 / N_{\rm ss}$ different initial values. For each cycle, we have a number of $N_{\rm ss}$ iterations (discrete transitions), and thus, $N_{\rm ss}$ values of q-indices. Therefore, the whole number of the values of q-indices for all the cycles is 2×10^5 for all the chosen values of $N_{\rm ss}$.

The probability distribution $P(q)$ of the whole number of 2×10^5 values of q-indices is constructed and plotted in Figure 7. In particular, in the panels (a)—(d), we plot the probability distribution $P(q)$ for different number of iterations, i.e., (a) $N_{\rm ss} = 2 \times 10$ (10^4 initial values), (b) $N_{\rm ss} = 2 \times 10^2$ (10^3 initial values), (c) $N_{\rm ss} = 2 \times 10^3$ (10^2 initial values), and (d) $N_{\rm ss} = 2 \times 10^4$ (10 initial values). The more iterations, the more widely distributed are the values. For iterations less than 2×10^3 (and keeping the same entropic step $\delta S = 10^{-4}$), the stationary states remain within the cavity, $q \in [q_{\rm Esc}, \frac{5}{3})$, and do not escape to the near-equilibrium region of $q \in [1, q_{\rm Esc})$ (Figures 7(a)–(c)). However, they do escape for a larger number of iterations, i.e., for $N_{\rm ss} = 2 \times 10^4$ (Figure 7(d)). In addition, we have found that the asymptotic behavior of $P(q)$ near equilibrium, $P(q) \sim e^{-2.45 M_q}$, and near q-frozen state, $P(q) \sim \frac{1}{1-M_q}$, respectively. The near-equilibrium region collects the stationary states that came from both the A- and D-branches inside the cavity, and this is the reason that in the plot of Figure 7(d) it appears as a small abrupt step at $q \cong q_{\rm Esc}$. Eventually, all the stationary states will move from the far-equilibrium $q \in [q_{\rm Esc}, \frac{5}{3})$ to the near-equilibrium region $q \in [1, q_{\rm Esc})$.

For the assumptions used in this simple numerical experiment, it takes about $n_{\rm q-F} \cong 2 \times (1.5 - S_{\rm Fund})/\delta S \cong 0.43/\delta S$ iterations for a stationary state to depart from the far-equilibrium to the near-equilibrium region. Here we assume that in the isentropic switching, states are equally likely to switch in both directions across the cavity and that a switch occurs on average every two time steps, giving the multiplier 2 in this expression. For $\delta S = 10^{-4}$, we have approximately a number of $n_{\rm q-F} \cong 4300$ iterations being spread inside the cavity of the near q-frozen state region (far-equilibrium region), out of $N_{\rm ss}$ total iterations. On the other hand, around $n_{\rm EQ} \cong [(S_{\rm EQ} - 1.5) + 2 \times (1.5 - S_{\rm Fund})]/\delta S \cong 2.15/\delta S$ iterations are needed for a stationary state to reach equilibrium. For $\delta S = 10^{-4}$, we have $n_{\rm EQ} \cong 21500$ out of $N_{\rm ss}$

total iterations. In fact, having $N_{ss} = 2 \times 10^4$ (Figure 7(d)), namely, $N_{ss} \cong n_{EQ}$, equilibrium ($q = 1$) is barely reached. Actually, our choice of $N_{ss} = 2 \times 10^4$ was based exactly on this fact, since the Maxwellian distributions have been observed in solar wind, but not that frequently.

We find that around $(n_{EQ} - n_{q-F})/n_{EQ} \cong 80\%$ of the stationary states depart from the cavity to the near-equilibrium region, accumulated close to the marginal state at equilibrium. On the other hand, around $n_{q-F}/n_{EQ} \cong 20\%$ of the stationary states stay in the cavity, while around the half of them, $\sim 10\%$, (because of the isentropic mechanism) are accumulated close to the margin of the q-frozen state. Therefore, the number of stationary states that are accumulated near equilibrium compared to those near the q-frozen state is $\sim$8:1, but the former is spread over an 8 times larger interval, $(q_{Esc} - 1)/(\frac{5}{3} - q_{Fund}) \cong 8 : 1$.

It is apparent now that both branches ultimately lead all the stationary states (under different dynamical procedures) to equilibrium. First, and after a sufficient time, one should observe the accumulated stationary states near the q-frozen state and near equilibrium. However, the respective dominant peaks, that is the sharp peak at the q-frozen state and the broad peak at equilibrium (see Figure 7(d)), do not constitute a permanent configuration. In contrast, the former is getting weaker, while the latter is getting stronger over the passage of time, because stationary states transit from the accumulation at the q-frozen state and escape from the cavity through the isentropic mechanism. Therefore, the transition of stationary states, under small constant augments of entropy (e.g., $\delta S = 10^{-4}$), affirms the gradual diversion of stationary states from the q-frozen state to equilibrium, and the relevant shifting of the probability distribution of particles to larger values of velocities (or energies).

7. CONCLUSIONS

In summary, the 10 major points developed in this paper are as follows.

1. *Arrangement of stationary states.* A spectrum-like arrangement of stationary states can be detectable within the framework of Tsallis statistical mechanics, where the values of the κ-index are in the interval $\kappa \in (\frac{3}{2}, \infty]$, or, the values of the q-index in the interval $q \in [1, \frac{5}{3})$. The first boundary value, i.e., $\kappa = \infty$ (or $q = 1$), is equilibrium, while the second boundary value defines the furthest stationary state from equilibrium, i.e., in a three-dimensional system $\kappa \to \frac{3}{2}$ (or $q \to \frac{5}{3}$).
2. *Isothermal and iso-metastability procedures.* The temperature T_q remains invariant for all the values of the q-index, so that different values of temperature do not specify different stationary states. Having identified each stationary state by the value of its q-index, we introduced a novel isothermal procedure that describes a system's transition into stationary states by varying the q-index, and showed how the variation of temperature can be realized in an "iso-metastability" procedure, in which the system remains in a fixed stationary state.
3. *Generalized zeroth law of thermodynamics for stationary states out of equilibrium.* "Two bodies that are in equilibrium *or the same non-equilibrium stationary state* with a third are in *the same stationary state* with each other." In the case of two contacting systems that are in the same stationary state, the heat will flow from the hotter to the colder, as in the classical case, but the governing definition of temperature is given uniquely by the physical temperature, T_q.

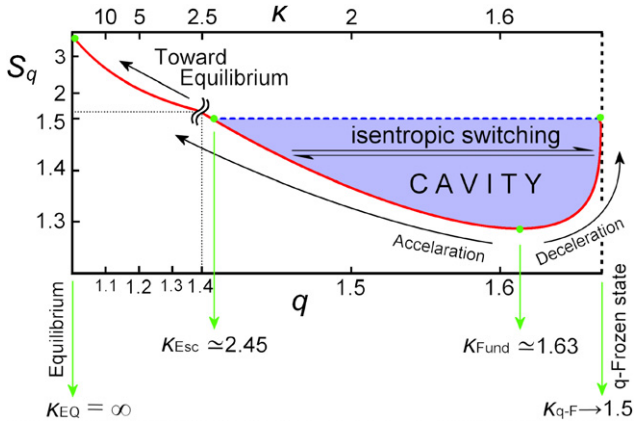

Figure 8. Tsallis entropy S_q, calculated for the Tsallis–Maxwellian distribution of velocities, is depicted with respect to the q- and κ-indices (second interpretation of the speed-scale parameter σ). We indicate the acceleration $\infty \geqslant \kappa \geqslant \kappa_{Fund}$ and deceleration $\kappa_{Fund} \geqslant \kappa > \frac{3}{2}$ branches; the isentropic switching that can take place between the two branches inside the cavity $\kappa_{Esc} \geqslant \kappa > \frac{3}{2}$; and the critical κ-indices corresponding to the extreme states of equilibrium $\kappa_{EQ} = \infty$ and the q-frozen state $\kappa_{q-F} \to \frac{3}{2}$, the escape point from the cavity, $\kappa_{Esc} \cong 2.45$ (separates the near-equilibrium $\infty \geqslant \kappa > \kappa_{Esc}$ from the far-equilibrium $\kappa_{Esc} \geqslant \kappa > \frac{3}{2}$ regions), and the fundamental state, $\kappa_{Fund} \cong 1.63$ (minimum entropy).

4. *q-Frozen state.* The q-frozen stationary state is described by a specific power-law probability distribution of velocities $P_{q-F}(w) \sim w^{-3}$, independent of the dimensionality f. We call this the q-frozen state, because it turns out that by approaching this state, the system behaves analogously to when the temperature decreases approaching the absolute zero.
5. *q-metastability, the "thermodynamic distance" of stationary states from equilibrium.* This universality that characterizes the q-frozen state, together with the fact that it is the furthest possible stationary state from equilibrium and can be referred to as 100% away from equilibrium, motivated us to define a measure of the "thermodynamic distance" of a stationary state from equilibrium. This is expressed in terms of the Tsallis entropic index q, and fulfills several defining conditions. We call this measure q-metastability, M_q, because the further from equilibrium a stationary state is, the more metastable states there are between it and equilibrium. Each stationary state lies between the extreme stationary states of equilibrium and the q-frozen state, characterized by q-metastability measure within the interval 0% and 100%.
6. *The critical values of the κ-index.* There are four special values of the κ-index that appear in space plasmas: the extreme values of $\kappa_{EQ} = \infty$ and $\kappa_{q-F} \cong 1.5$ that corresponds to the specific stationary states at equilibrium and the q-frozen state, respectively; the value of $\kappa_{Fund} \cong 1.63$ that is the fundamental state; and the value of $\kappa_{Esc} \cong 2.45$ that is the escape state which separates the stationary states that distributed near equilibrium, $\infty \geqslant \kappa > \kappa_{Esc}$, from those near the q-frozen state, $\kappa_{Esc} \geqslant \kappa > \frac{3}{2}$ (see Table 1).
7. *Entropy of a system in a stationary state.* The entropy of a stationary metastable state is expressed in terms of the κ-index (or equivalently, in terms of the q-index or the measure M_q). We identify two possible solutions for the entropy as a function of q, depending on whether one sets the speed-scale parameter, σ, by relating it to the physical temperature, T_q, or the temperature-like parameter in Tsallis statistics, the Lagrangian, T. Using the second of

these, we show that while the entropy increases monotonically with the κ-index in $\infty \geqslant \kappa > \kappa_{\rm Esc}$, it is non-monotonic in $\kappa_{\rm Esc} \geqslant \kappa > \frac{3}{2}$, exhibiting a minimum value at $\kappa_{\rm Fund} \cong 1.63$, that is quite close to the final value of $\kappa_{\rm q-F} \to \frac{3}{2}$. The whole entropic graph can be separated into the two monotonic *A*- and *D*- branches. As the entropy increases, the value of the κ-index increases along the *A*-branch, while it decreases along the *D*-branch (Figure 8). The probability distribution is shifted toward larger or smaller velocities (higher or lower energies) by increasing or decreasing the κ-index, and exhibiting a phenomenological acceleration and deceleration of particles, respectively.

8. *Prediction of the critical values of κ-index.* Both the solutions of entropy of stationary states, accordingly to the two possible interpretations of the speed-scale parameter, reveal the detailed paths by which the transition of stationary states evolves toward equilibrium. However, the specific dynamical scenario of the second interpretation naturally provides the special values of the κ-index that are frequently observed in space plasmas (listed in 6 above). For this reason and for all the arguments exposed in Section 5.1, we believe that this scenario may be applicable in space plasmas.
9. *The characteristic difference equation of stationary states transitions.* The evolution of the probability distribution of velocities can be characterized by a difference equation of the q-indices (or equivalently, of the κ-indices or measures M_q) that replaces the differential equations that usually describes space plasmas (e.g., Vlasov–Maxwell's, Parker's, etc.). This is a specific recurrent relation that maps a current value of the q-index, q_n, to its sequential value, q_{n+1}, with the continuous time t, being replaced by the discrete serial number, n, that counts the sequential stationary states. The key point in this relation is the specific way that the entropy varies between the stationary states. This approach highlights the hereby developed basic concept that space plasmas systems are mostly governed by metastable stationary states, while the relevant transition times of the departures and arrivals of the system to each one of these sequential stationary states are much less important. Therefore, the whole information for the dynamics of the system is included in the sequential stationary states, namely, in the discrete time dependence of q-indices and their characteristic difference equation.
10. *The five stages of the stationary states transitions made possible under the second interpretation:*

    The intermediate transitions toward the q-frozen state. Starting from stationary states near the fundamental state, interior (irreversible) procedures that increase the entropy of stationary states move the system either toward equilibrium (entropy increases along the *A*-branch) or toward the q-frozen state (entropy increases along the *D*-branch).

    The isentropic switching and its importance. The stationary states inside the cavity can be affected by an isentropic switching between the two branches. In this way, the transitions of stationary states toward the q-frozen state along the *D*-branch can alter to the transitions toward equilibrium along the *A*-branch, and vice versa. This mostly affects the stationary states that are quite close to the q-frozen state, for which an increase of the entropy leads to stationary states out and near the edge of the cavity $\kappa > \kappa_{\rm Esc}$.

    The double role of the q-frozen state. In intermediate times, the stationary states do not escape yet from the cavity, but instead accumulate near the q-frozen state. This is mostly the case when the interior (irreversible) procedures that increase the entropy of stationary states are rare, e.g., in the quite times of solar wind. However, after a sufficient number of transitions the stationary states finally escape from the cavity, because of the isentropic mechanism. Then, the particles depart from the q-frozen state ($M_q \to 100\%$) and transit toward equilibrium ($M_q = 0\%$).

    The final transitions toward equilibrium. The stationary states ultimately transit toward equilibrium, either directly, as entropy increases along the *A*-branch, or indirectly, as entropy increases along the *D*-branch and after an isentropic switching that leads the stationary states to escape from the cavity. In other words, the particles depart from the q-frozen state, i.e., the most distant stationary state from equilibrium ($M_q \to 100\%$), and transit to the specific stationary state at equilibrium ($M_q = 0\%$).

    The rejuvenation of entropy. External factors that can decrease the entropy of the system move it into a different stationary state, closer to the fundamental state. In the case of solar wind, for example, newly formed pick-up ions may play just such a role because their motion is highly ordered, and thus the entropy of stationary states decreases.

The work presented here is a generalization of the Maxwell's kinetic theory for collisionless plasmas out of equilibrium. Namely, the energy is given simply by the kinetic energy, while any other extra dynamical contributions (e.g., long range interactions) are ignored. The previously only stationary state at equilibrium now degenerates to a spectrum-like arrangement of stationary states, in which the identity of each state is interpreted by its specific value of the κ-index (or equivalently, the q-index, or the measure M_q). The furthest stationary state from equilibrium, the q-frozen state ($\kappa_{\rm q-F} \cong 1.5$, for three-dimensional systems) becomes an attractor, likely accounting for this commonly observed value in space.

The detection of the critical values of the κ-index in space and other plasmas is interesting. It will be motivating to continue the search for new observations and see which interpretation is supported, in laboratory plasmas and non-plasma systems, especially the fundamental $\kappa_{\rm Fund} \cong 1.63$ and escape value $\kappa_{\rm Esc} \cong 2.45$ that have important roles in the certain dynamics of the stationary states transitions, according to the second interpretation. Due to the isentropic switching, the escape value $\kappa_{\rm Esc} \cong 2.45$ is related to the value of the q-frozen state, $\kappa_{\rm q-F} \to \frac{3}{2}$, and vice versa. In fact, it may be a challenge to experimentally detect and verify the entropic switching for values in the cavity, $\kappa_{\rm Esc} \geqslant \kappa > \frac{3}{2}$.

Finally, we stress that something must be playing the role of decreasing the entropy of stationary states in space plasmas, and driving the outer heliospheric states back toward the fundamental. We believe that the increasing influence of pick-up ions is the most likely source of this re-ordering of the plasma and that this procedure, and the competition between this reordering and the natural progression of increasing entropy, likely play a critical element in defining space plasmas.

We are grateful to S. M. Krimigis and K. Dialynas for providing us with the data of κ-indices of particle distributions in the Saturnian magnetosphere from the MIMI suite onboard Cassini.

George Livadiotis gratefully acknowledges useful discussions with C. Tsallis related to the physical temperature and the relevant generalization of the zeroth law of thermodynamics. This work was funded in part by NASA's *Ulysses*, *ACE*, and IBEX projects.

REFERENCES

Abe, S. 1999, Physica A, 269, 403
Abe, S., Martínez, S., Pennini, F., & Plastino, A. 2001, Phys. Lett. A, 281, 126
Aharonian, F., et al. 2006, Nature, 440, 1018
Arnaud, K. A., et al. 1985, MNRAS, 217, 105
Aschwanden, M. J., et al. 2000, ApJ, 535, 1047
Bazarghan, M., Safari, H., Innes, D. E., Karami, E., & Solanki, S. K. 2008, A&A, 492, L13
Beck, C., & Schlogl, F. 1993, Thermodynamics of Chaotic Systems (Cambridge: Cambridge Univ. Press)
Benz, A. O. 2004, in Proc. IAU Symp. 219, Stars as Suns: Activity, Evolution, and Planets, ed. A. K. Dupree & A. O. Benz (San Francisco, CA: ASP), 461
Burlaga, L. F., & Viñas, A. F. 2005, Physica A, 356, 375
Chakrabarti, S. K., & Titarchuk, L. G. 1995, ApJ, 455, 623
Charbonneau, P., McIntosh, S. W., Liu, H. L., & Bogdan, T. J. 2001, Sol. Phys., 203, 321
Chotoo, K., et al. 2000, J. Geophys. Res., 105, 23107
Christon, S. P. 1987, Icarus, 71, 448
Collier, M. R., Hamilton, D. C., Gloeckler, G., Bochsler, P., & Sheldon, R. B. 1996, J. Geophys. Res., 23, 1191
Crosby, N. B., Aschwanden, M. J., & Dennis, B. R. 1993, Sol. Phys., 143, 275
Dayeh, M. A., Desai, M. I., Dwyer, J. R., Rassoul, H. K., Mason, G. M., & Mazur, J. E. 2009, ApJ, 693, 1588
Decker, R. B., Krimigis, S. M., Roelof, E. C., Hill, M. E., Armstrong, T. P., Gloeckler, G., Hamilton, D. C., & Lanzerotti, L. J. 2005, Science, 309, 2020
Desai, M. I., et al. 2004, ApJ, 611, 1156
Dialynas, K., Krimigis, S. M., Mitchell, D. G., Hamilton, D. C., Krupp, N., & Brandt, P. C. 2009, J. Geophys. Res., 114, A01212
Dialynas, K., et al. 2008, AGU Fall Meeting 2008, abstract, P11B-1269
Elaydi, S. 2005, An Introduction to Difference Equations (New York: Springer)
Ferri, G., Martínez, S., & Plastino, A. 2005, Physica A, 347, 205
Fisk, L. A., & Gloeckler, G. 2006, ApJ, 640, L79
Fuselier, S. A., et al. 2009, Science, 326, 962
Göğüş, E., et al. 1999, ApJ, 526, L93
Hammond, C. M., et al. 1996, J. Geophys. Res., 100, 7881
Heerikhuisen, J., Pogorelov, N. V., Florinski, V., Zank, G. P., & le Roux, J. A. 2008, ApJ, 682, 679
Hellberg, M. A., Mace, R. L., Baluku, T. K., Kourakis, I., & Saini, N. S. 2009, Phys. Plasmas, 16, 094701
Ilovaisky, S. A., Chevalier, C., Motch, C., & Chiappetti, L. 1986, A&A, 164, 67
Kanamori, H. 1978, Nature, 271, 411
Kashyap, V. L., Drake, J. J., Güdel, M., & Audard, M. 2002, ApJ, 580, 1118
Kifune, T., et al. 1995, ApJ, 438, L91
Krennrich, F., et al. 1999, ApJ, 511, 149
Lee, M. A., & Ip, W.-H. 1987, J. Geophys. Res., 92, 11041
Leubner, M. P. 2002, Ap&SS., 282, 573
Leubner, M. P. 2004a, ApJ, 604, 469
Leubner, M. P. 2004b, Phys. Plasmas, 11, 1308
Livadiotis, G., & McComas, D. 2009, J. Geophys. Res. A, 114, 11105
Mann, G., Classen, H. T., Keppler, E., & Roelof, E. C. 2002, A&A, 391, 749
Marsch, E. 2006, Living Rev. Sol. Phys., 3, 1
Mason, G. M., et al. 2008, ApJ, 678, 1458
Mauk, B. H., Krimigis, S. M., Keath, E. P., Cheng, A. F., Armstrong, T. P., Lanzerotti, L. J., Gloeckler, G., & Hamilton, D. C. 1987, J. Geophys. Res., 92, 15283
Mauk, B. H., et al. 2004, J. Geophys. Res., 109, A09S12
McComas, D. J., et al. 2009, Science, 326, 959
McIntosh, S. W., & Charbonneau, P. 2001, ApJ, 563, L165
McIntosh, S. W., et al. 2002, Phys. Rev. E., 65, 046125
McNutt, R. L., Jr., Lyon, J., & Goodrich, C. C. 1999, J. Geophys. Res., 104, 14803
Milovanov, A. V., & Zelenyi, L. M. 2000, Nonlin. Process. Geophys., 7, 211
Miyamoto, S., Kimura, K., Kitamoto, S., Dotani, T., & Ebisawa, K. 1991, ApJ, 383, 784
Nieves-Chinchilla, T., & Viñas, A. F. 2008a, J. Geophys. Res. A, 113, 02105
Nieves-Chinchilla, T., & Viñas, A. F. 2008b, Geofís. Int., 47, 245
Norman, J. P., Charbonneau, P., McIntosh, S. W., & Liu, H. L. 2001, ApJ, 557, 891
Parnell, E. N., & Jupp, P. E. 2000, ApJ, 529, 554
Pauluhn, A., & Solanki, S. K. 2007, A&A, 462, 311
Prato, D., & Tsallis, C. 1999, Phys. Rev. E., 60, 2398
Prested, C., et al. 2008, J. Geophys. Res. A, 113, 06102
Raadu, M. A., & Shafiq, M. 2007, Phys. Plasmas, 14, 012105
Rama, S. K. 2000, Phys. Lett. A, 276, 103
Sagdeev, R. Z., Shapiro, V. D., Shevchenco, V. I., & Szego, K. 1986, Geophys. Res. Lett., 13, 85
Saito, S., Forme, F. R. E., Buchert, S. C., Nozawa, S., & Fujii, R. 2000, Ann. Geophys., 18, 1216
Sato, Y., Shimada, E., Ohta, I., Tasaka, S., & Tanaka, S. 1985, J. Phys. Soc. Japan, 54, 4502
Schippers, P., et al. 2008, J. Geophys. Res., 113, A07208
Schreier, E., Gursky, H., Kellogg, E., Tananbaum, H., & Giacconi, R. 1971, ApJ, 170, L21
Schroedter, M., et al. 2005, ApJ, 634, 947
Schwadron, N. A., et al. 2009, Science, 326, 966
Shimizu, T. 1995, PASJ, 47, 251
Shizgal, B. D. 2007, Ap&SS, 312, 227
Silva, R., Plastino, A. R., & Lima, J. A. S. 1998, Phys. Lett. A, 249,, 401
Steffl, A. J., Bagenal, F., & Stewart, A. I. F. 2004, Icarus, 172, 91
Syunyaev, R. A., et al. 1994, Astron. Lett., 20, 777
Toral, R. 2003, Physica A, 317, 209
Tsallis, C. 1988, J. Stat. Phys., 52, 479
Tsallis, C. 1999, Braz. J. Phys., 29, 1
Tsallis, C. 2009, Introduction to Nonextensive Statistical Mechanics (New York: Springer)
Tsallis, C., Levy, S. V. F., Souza, A. M. C., & Maynard, R. 1995, Phys. Rev. Lett., 75, 3589
Tsallis, C., Mendes, R. S., & Plastino, A. R. 1998, Physica A, 261, 534
Vasyliūnas, V. M. 1968, J. Geophys. Res., 73, 2839
Venters, T. M., & Pavlidou, V. 2007, ApJ, 666, 128
Von Montigny, C., et al. 1995, ApJ, 440, 525
Wang, C.-P., Lyons, L. R., Chen, M. W., Wolf, R. A., & Toffoletto, F. R. 2003, J. Geophys. Res., 108, 1074
Wang, Q. A., Nivanen, L., Le Méhauté, A., & Pezeril, M. 2002, J. Phys. A, 35, 7003
Yamano, T. 2002, Physica A, 305, 486
Yashiro, S., Akiyama, S., Gopalswamy, N., & Howard, R. A. 2006, ApJ, 650, L143
Yoon, P. H., Rhee, T., & Ryu, C.-M. 2006, J. Geophys. Res. A, 111, 09106
Zilbersher, D., & Gedalin, M. 1997, Planet. Space Sci., 45, 693
Zouganelis, I., Maksimovic, M., Meyer-Vernet, N., Lamy, H., & Issautier, K. 2004, ApJ, 606, 542